

1
2
3
4 **Neurotrophin gene augmentation by electrotransfer to improve cochlear implant**
5 **hearing outcomes**
6
7
8

9 Jeremy L. Pinyon¹, Georg von Jonquieres¹, Edward N. Crawford¹, Mayryl Duxbury¹, Amr Al
10 Abed², Nigel H. Lovell², Matthias Klugmann¹, Andrew K. Wise³, James B. Fallon³, Robert K.
11 Shepherd³, Catherine S. Birman^{4,5}, Waikong Lai⁴, David McAlpine⁶, Catherine McMahon⁶,
12 Paul M. Carter⁷, Ya Lang Enke⁷, James F. Patrick⁷, Anne G.M. Schilder⁸, Corinne Marie⁹,
13 Daniel Scherman⁹, Gary D. Housley¹
14
15
16
17

18 ¹Translational Neuroscience Facility & Department of Physiology, School of Medical
19 Sciences, UNSW Sydney, New South Wales, Australia; ²The Graduate School of Biomedical
20 Engineering, UNSW, Sydney, New South Wales, Australia; ³Bionics Institute, St Vincent's
21 Hospital, Melbourne, Australia, the Department of Medical Bionics, University of Melbourne,
22 Melbourne, Australia, Department of Otolaryngology, University of Melbourne, Melbourne,
23 Australia; ⁴Department of Otolaryngology, Royal Prince Alfred Hospital, Camperdown, NSW,
24 Australia; ⁵The Sydney Cochlear Implant Centre, Royal Institute of Deaf and Blind Children,
25 Gladesville, NSW, Australia Department of Linguistics, Faculty of Human Sciences,
26 Macquarie University, North Ryde, Australia; ⁶The Hearing Hub, Macquarie University,
27 Sydney, Australia, The HEARing Cooperative Research Centre, Melbourne, Australia;
28 Cochlear Ltd, Sydney, Australia; ⁸Ear Institute, University College London, London, United
29 Kingdom; ⁹Laboratory of Chemical and Biological Technologies for Health, Université Paris
30 Descartes, Sorbonne-Paris-Cité, F-75006 Paris, France, CNRS, UTCBS UMR 8258, F-75006
31 Paris, France, Chimie ParisTech, PSL Research University, UTCBS, F-75005 Paris, France,
32 INSERM, UTCBS U 1267, F-75006 Paris, France.
33
34
35

36 **Keywords:** Brain derived neurotrophic factor; neurotrophin-3; bionic array directed gene
37 electrotransfer; auditory nerve fibre regeneration; gene therapy; sensorineural hearing loss.
38
39
40
41

42 *Address for correspondence:*

43 Gary Housley

44 Department of Physiology

45 School of Medical Sciences

46 UNSW Sydney

47 NSW 2052

48 Australia

49 Email: g.housley@unsw.edu.au

50 Tel: +61 2 93851057
51
52
53
54
55
56
57
58
59

60
61
62 **Abstract**
63
64

65 This Review outlines the development of DNA-based therapeutics for treatment of hearing
66 loss, and in particular, considers the potential to utilize the properties of recombinant
67 neurotrophins to improve cochlear auditory (spiral ganglion) neuron survival and repair. This
68 potential to reduce spiral ganglion neuron death and indeed re-grow the auditory nerve fibres
69 has been the subject of considerable pre-clinical evaluation over decades with the view of
70 improving the neural interface with cochlear implants. This provides the context for discussion
71 about the development of a novel means of using cochlear implant electrode arrays for gene
72 electrotransfer. Mesenchymal cells which line the cochlear perilymphatic compartment can be
73 selectively transfected with (naked) plasmid DNA using array - based gene electrotransfer,
74 termed 'close-field electroporation'. This technology is able to drive expression of brain
75 derived neurotrophic factor (BDNF) in the deafened guinea pig model, causing re-growth of
76 the spiral ganglion peripheral neurites towards the mesenchymal cells, and hence into close
77 proximity with cochlear implant electrodes within scala tympani. This was associated with
78 functional enhancement of the cochlear implant neural interface (lower neural recruitment
79 thresholds and expanded dynamic range, measured using electrically - evoked auditory
80 brainstem responses). The basis for the efficiency of close-field electroporation arises from the
81 compression of the electric field in proximity to the ganged cochlear implant electrodes. The
82 regions close to the array with highest field strength corresponded closely to the distribution of
83 bioreporter cells (adherent human embryonic kidney (HEK293)) expressing green fluorescent
84 reporter protein (GFP) following gene electrotransfer. The optimization of the gene
85 electrotransfer parameters using this cell-based model correlated closely with *in vitro* and *in*
86 *vivo* cochlear gene delivery outcomes. The migration of the cochlear implant electrode array-
87 based gene electrotransfer platform towards a clinical trial for neurotrophin-based
88 enhancement of cochlear implants is supported by availability of a novel regulatory compliant
89 mini-plasmid DNA backbone (pFAR4; plasmid Free of Antibiotic Resistance v.4) which could
90 be used to package a 'humanized' neurotrophin expression cassette. A reporter cassette
91 packaged into pFAR4 produced prominent GFP expression in the cat basal turn perilymphatic
92 scalae, which closely models the human cochlea. More broadly, close-field gene electrotransfer
93 may lend itself to a spectrum of potential DNA therapeutics applications benefitting from
94 titratable, localized, delivery of naked DNA, for gene augmentation, targeted gene regulation,
95 or gene substitution strategies.
96
97
98
99
100
101
102
103
104
105
106
107
108
109
110
111
112
113
114
115
116
117
118

1. Overview

1.1. Inner ear gene delivery

The translational potential of gene therapy in the inner ear is developing considerable prominence within the burgeoning domain of hearing therapeutics. This is founded upon successes in pre-clinical models that have utilized directed manipulation of gene expression to investigate developmental and physiological processes of hearing and balance at the molecular level. Modalities used for expression of recombinant proteins include ballistics ('gene gun'-based delivery of gold particles coated with DNA) (Belyantseva, 2009; Zhao et al., 2012), lipofectamine-based transduction, and replication-deficient viral-vector-based approaches (typically adenovirus, or adeno-associated virus (AAV)) (Akil et al., 2012; Kelley, 1997; Pan et al., 2013; Wise et al., 2010). Targeting of gene expression is highly variable, being regulated to some extent by use of promoters biasing translation of recombinant proteins to subsets of the highly differentiated cell types in the inner ear (Praetorius et al., 2010). In the case of viral vectors, selection between different viral capsid serotypes has a major effect on cell tropism, for example use of AAV1 enabled inner hair cell-specific expression of vesicular glutamate transporter-3 (VGLUT3) to restore hearing in VGLUT3 null mice (Akil et al., 2012), while use of the Anc80L65 serotype enables transfection of outer hair cells alongside inner hair cells (Landegger et al., 2017). In the vestibular system, the Ad28 serotype of adenovirus has been shown to selectively enable expression in supporting cells (Schlecker et al., 2011). Electroporation offers an alternative approach for inner ear gene delivery that has largely been constrained to *in vitro* tissue culture studies and *in utero* gene transfer (Driver et al., 2010; Wang et al., 2012). Typically plate electrodes are placed across the target tissue and a brief train of voltage pulses is used to drive plasmid DNA incorporating various expression cassettes into inner ear cells via conventional 'open-field' electroporation (Xiong et al., 2014), for example transfecting organ of Corti hair cells and supporting cells. Directed electrotransfer of naked DNA to targets within the cochlea via 'close-field' electroporation, where the electrodes are in a contiguous array, is proving highly effective both *in situ* and *in vivo* (Pinyon et al., 2018; Pinyon et al., 2014; Shepherd et al., 2014).

Investment in hearing gene therapy by industry will focus on rectification of monogenic disorders underlying profound loss of hearing (and / or balance), as well as rescue of acquired sensori-neural hearing loss (Lustig et al., 2012). A case in point is the first hearing gene therapy clinical trial supported by a consortium sponsored by Novartis Pharmaceuticals (Pharmaceuticals, 2019), which is directed to restore moderate to severe acquired hearing loss. This program utilizes an adenoviral vector (Ad(5)GFAP.HATH 1.11D; CGF166) encoding the

178
179
180 human atonal homolog-1 transcription factor (referred to as Hath1, and in animals studies as
181 Atoh1, also known as Math1), delivered into the scala vestibuli cochlear perilymph via
182 injection through the stapedius bone and oval window membrane (Brough et al., 2016). This
183 was founded upon pre-clinical studies of models of hair cell loss where Atoh1 expression
184 successfully drove trans-differentiation of supporting cells into new sensory hair cells, with
185 improvement in hearing and balance function (Baker et al., 2009; Husseman et al., 2009;
186 Izumikawa et al., 2005; Kawamoto et al., 2003; Schlecker et al., 2011). This next generation
187 hearing therapeutics, which seeks to restore sound transduction by creating new cochlear hair
188 cells and establishing new auditory synapses with spiral ganglion neurons, is at the threshold
189 of a quantum leap from current clinical management of inner ear disorders. However, such
190 powerfully interventional molecular therapies require vigilance with regard to impacts on the
191 complex signal transduction pathways both within and beyond the inner ear.
192
193
194
195
196
197
198
199
200

201 **1.2 A rationale for neurotrophic factor gene therapy to enhance the cochlear implant**

202 While moderate - to - severe levels of hearing loss can be treated by hearing aids, those
203 with profound hearing disability are increasingly benefitting from cochlear implants, with well
204 in excess of half a million people accessing this advanced medical bionics technology. In this
205 domain, neurotrophin delivery integrated into the cochlear implantation procedure has been
206 explored as a means of enhancing hearing performance with the ‘Bionic Ear’ (Budenz et al.,
207 2012; Hendricks et al., 2008; Wise et al., 2016). This concept has largely been pursued in pre-
208 clinical animal models using direct delivery of the neurotrophins to the cochlea (Landry et al.,
209 2013; Leake et al., 2013; Miller et al., 2007; Ramekers et al., 2012; Wise et al., 2005), or by
210 use of locally delivered viral vectors encoding these neurotrophins (Ramekers et al., 2012;
211 Shibata et al., 2010; Wise et al., 2010). The pre-clinical studies utilising gene delivery
212 approaches are complemented by a relatively smaller group of studies evaluating cell-based
213 therapies, utilising encapsulated cells, such as choroid plexus-derived cells, which are known
214 to produce a range of neurotrophic factors (Fransson et al., 2018; Pettingill et al., 2011; Wise
215 et al., 2011). Studies in deafened cats with long-term osmotic minipump delivery, and in guinea
216 pigs with adenovirus-based brain derived neurotrophic factor (BDNF) and neurotrophin-3 (NT-
217 3) delivery to scala media respectively, showed improved spiral ganglion neuron survival and
218 significant re-generation of the spiral ganglion neurites, albeit with some over-extension of the
219 fibres. While improved proximity between the cochlear implant electrodes and the peripheral
220 auditory nerve fibres ‘closes the neural gap’ and improves the neural interface, excessive
221 extension of the fibres has the potential to degrade the tonotopically-related neural recruitment
222
223
224
225
226
227
228
229
230
231
232
233
234
235
236

237
238
239 (Leake et al., 2013). However, there is some evidence from the viral vector delivery studies
240 that the extension of the spiral ganglion neurites may be directed outwards through the osseous
241 spiral lamina and along the basilar membrane towards the cells producing the recombinant
242 BDNF (Shibata et al., 2010). This tropism can be exploited with targeted gene delivery, to draw
243 the auditory fibres to the cochlear implant array. While high efficiency and long-duration of
244 expression of viral vector-based gene therapy is attractive in many applications, it may be
245 problematic from a safety view-point with respect to recombinant neurotrophin expression
246 cassette delivery to the cochlea. Several studies have shown that delivery of microlitre
247 quantities of AAV vector to the perilymphatic compartment of the cochlea can result in
248 significant off-target “leakage” of expression. For example, in the case of a translational model
249 to restore hearing and balance in an Usher syndrome 1c mouse model, delivery of an Anc80L65
250 AAV-harmonin-b1 vector unilaterally via the cochlear round window membrane resulted in
251 rescue of sound transduction in the untreated cochlea (Pan et al., 2017); evidently the virus
252 reached there via the cochlear fluid, including perilymph within the cochlear aqueduct that
253 connects to the subarachnoid space cerebral spinal fluid compartment, and beyond. Vestibular
254 dysfunction was also rescued in these studies, highlighting the contiguous nature of the
255 perilymphatic compartments in the inner ear. The potential detrimental impact of off-target
256 AAV transfer to the CNS from the cochlea has been confirmed in another neonatal mouse study
257 using a glial-derived neurotrophic factor (GDNF) – expressing AAV-5 vector (Akil et al.,
258 2018). This study demonstrated spread of the AAV5-hGDNF vector from the cochlea to the
259 CNS and spiral cord, presumably via the cochlea aqueduct, and this was associated with
260 significant neurological dysfunction linked to broad loss of cerebellar Purkinje neurons,
261 centrally-mediated hearing loss and retarded growth correlated with the AAV5-hGDNF vector
262 titre (Akil et al., 2018). While it might be argued that patency of the cochlear aqueduct is not
263 comparable in human cochlear implant candidates, spread of active viral particles is
264 nevertheless a significant risk. Directed delivery of gene cassettes encoded by naked DNA to
265 the cochlea, which is achievable using cochlear implant array – based electrotransfer, mitigates
266 concerns linked to such viral vector off-target actions and may enable latent gene therapy
267 applications.

268
269
270
271
272
273
274
275
276
277
278
279
280
281
282
283
284
285
286
287
288
289
290
291
292
293
294
295

The context of establishing a neurotrophin gene therapy strategy for engaging with sensorineural hearing loss also warrants reflection on species-specific, developmental, and injury status with respect to expression of neurotrophins and their receptors in the cochlea. For example, it is known that in the rodent, the weighting of expression of BDNF and NT-3 changes with cochlear maturation, where BDNF declines but NT-3 levels are sustained, while all

296
297
298
299
300
301
302
303
304
305
306
307
308
309
310
311
312
313
314
315
316
317
318
319
320
cognate receptors (TrkB for BDNF, TrkC for NT-3 and p75^{ntr}, which transduces both BDNF and NT-3 at low affinity) are maintained by the spiral ganglion neurons (review by (Ramekers et al., 2012)). In the mouse cochlea, NT-3/TrkC signalling supports development of the basal-mid cochlear innervation of hair cell innervation, while BDNF/TrkB signalling supports apical hair cell innervation. This base – apex gradient of NT-3 expression (by inner hair cells) reverses in the adult, while the TrkB/TrkC spiral ganglion expression, remains homogenous (Ramekers et al., 2012). Signalling via TrkB/ TrkC invokes tyrosine kinase activation and complex phosphorylation-dependent processes which include phospholipase C activation driving Ca²⁺ store release and Ca²⁺ entry. The latter contributes to axon guidance, established for BDNF in the brain and cochlea, which is likely mediated by PLC-DAG dependent activation of canonical transient receptor potential (TRPC) channels (Li et al., 2005). Consistent with this, TRPC3 immunolabelling is pronounced in mouse and guinea pig spiral ganglion neurons, particularly in the peripheral neurites during the crucial neonatal window for innervation of the hair cells (Phan et al., 2010; Tadros et al., 2010), and is then elevated in the soma in adults.

321
322
323
324
325
326
327
328
329
330
331
332
333
334
335
336
337
In animal models, loss of cochlear hair cells associated reduction in neurotrophin production, causes atrophy of the peripheral spiral ganglion neurites in the osseous spiral lamina and subsequent progressive death of the neurons over periods of weeks to months (Fransson et al., 2017). Fortunately the human cochlea exhibits considerable resilience, with retention of much of the spiral ganglion neuron population for decades following loss of the hair cells (Leake et al., 1991; Nadol, 1997). This makes cochlear implants tenable as the primary treatment for profound hearing loss, and with regard to hearing therapeutics, makes treatment with neurotrophins attractive with regard to the bionic ear interface, both by mitigating progressive loss of spiral ganglion neurons, and if directed regulated re-growth towards the cochlear implant electrode array can be achieved, then finer control of neural recruitment may be possible, improving hearing performance.

338
339
340
341
342
343
344
345
346
347
348
349
350
351
352
353
354
Cochlear neurotrophin treatment has been broadly tested in deafened animal models with regard to cochlear implant performance. While characterisation of the extent of peripheral neurite regrowth is problematic, spiral ganglion neuron rescue by neurotrophin delivery has been examined with regard to measures such as electrically-evoked auditory brainstem response (eABR) thresholds and input/output functions. Findings from the acutely deafened guinea pig model with close-field BDNF gene electrotransfer outlined below (Pinyon et al., 2014), suggest that BDNF-induced improvement in spiral ganglion neuron health, measured by greater survival, increased soma cross-sectional area, and constrained peripheral neurite extension, do indeed confer improvements in control of cochlear implant- driven neural

355
356
357 recruitment. However, clinical evidence that spiral ganglion survival and retention of auditory
358 nerve fibres within the osseous spiral lamina correlates with hearing outcomes of cochlear
359 implant subjects is equivocal. For example, an early study (Nadol et al., 2001) reported that
360 spiral ganglion neuron counts were negatively correlated with single-syllable word recognition
361 in eight cases with electrode array-type implants, and there was no difference in neuron survival
362 relative to the opposite (non-implanted) cochleae. The latter in particular contrasts with the
363 reported improved survival of spiral ganglion neurons with electrical stimulation alone in a
364 deafened cat study (Leake et al., 1991), cautioning translational inferences from animal models.
365 Data comparing word recognition scores via left and right ears for bilaterally implanted
366 subjects, against post-mortem spiral ganglion neuron counts for six individuals clearly
367 demonstrated a positive correlation (Seyyedi et al., 2014). This has been supported by a study
368 across seventeen subjects which considered CNC word scores and spiral ganglion neuron
369 counts in conjunction with confounders such as cochlear implantation - induced neo-
370 osteogenesis (negative) and fibrosis (no effect) (Kamakura et al., 2016).

371
372 With regard to clinical application of neurotrophins with the aspiration of enhancing
373 cochlear implant performance, translational questions with finer granularity abound. For
374 example, neurotrophin treatment alongside cochlear implants may alter the expression and
375 properties of ion channels key to action potential initiation and propagation, which would
376 therefore impact on the auditory coding and hence central auditory processing. In many cases
377 the knowledge gained by undertaking a first-in-human trial is needed to provide the definitive
378 insights which currently remain unanswered, or unanswerable in pre-clinical models.
379
380

381 **2. Cochlear implant electrode array - based gene electrotransfer' for localized gene** 382 **delivery**

383 **2.1. Background to gene electrotransfer**

384
385 There has been a frameshift in understanding of pulsed electric field-based DNA
386 transfer in recent years, with studies showing that electroporation is a misnomer in that plasmid
387 DNA is too large to cross into cells through transiently generated pores in the plasma
388 membrane, with associated electrophoretic translocation of the negatively charged DNA.
389 Rather, it is now recognised that unlike small RNA and DNA oligonucleotide molecules, and
390 fluorescent molecules such as propidium iodide, that migrate through these temporary
391 membrane pores, plasmid DNA, which is MDa in size and approaches a hundred nm in
392 diameter, is largely taken up by cells by active processes. Thus, the effect of the train of electric
393
394
395
396
397
398
399
400
401
402
403
404
405
406
407
408
409
410
411

414
415
416
417
418
419
420
421
422
423
424
425
426
427
428
429
430
431
432
433
434
435
436
437
438
439
440
441
442
443
444
445
446
447
448
449
450
451
452
453
454
455
456
457
458
459
460
461
462
463
464
465
466
467
468
469
470
471
472

pulses that achieves such electroporation is of sufficient electric field strength that it drives the physical adherence of (plasmid) DNA to the cathode-facing surface of cells. This achieves inclusion of many thousands of these DNA molecules onto the plasma membrane, with internalization through endocytosis and pinocytotic mechanisms (Escoffre et al., 2011; Rosazza et al., 2016a; Rosazza et al., 2016b). The majority of these exogenous DNA molecules are then eliminated within lysosomes and by endonuclease activity, but a small fraction of the plasmid DNA (probably hundreds of copies) are transported to the nuclear pores, exiting from the transport vesicles and becoming established as extra-chromosomal (episomal) DNA. The episomal DNA is then transcribed to produce mRNA encoding the recombinant protein(s) (Pinyon et al., 2018). This plasmid DNA is characteristically resistant to degradation and after achieving detectable translation within a few hours, may support expression for many months (Wong et al., 2015). This process is therefore now more frequently referred to as DNA electrotransfer rather than electroporation. Key parameters for efficient expression of recombinant proteins using DNA electrotransfer tend to be related to the intrinsic biophysics of the gene delivery process. These include the starting plasmid DNA concentration and the magnitude and duration of the electric field. With regard to the former, plasmid DNA is typically delivered to cells in unitary $\mu\text{g}/\mu\text{l}$ concentrations (viscosity becoming a limiting feature with concentrations greater than $\sim 3 \mu\text{g}/\mu\text{l}$, usually in a dilute buffered saline solution). Electric pulse parameters used for gene delivery are typically hundreds of volts for tens of milliseconds, to generate voltage gradients (electric fields) that are in the range of 300 - 1000 V/cm (30 - 100 mV/ μm) (Rosazza et al., 2016b). The requirement for these high voltages for conventional open-field electroporation can result in potential tissue damage due to local ohmic heating and irreversible dielectric breakdown (Lacković et al., 2009).

2.2. Validation of BaDGE® for *in vitro* and *in vivo* directed gene delivery

While conventional open-field electroporation has been employed for *in vitro* gene delivery to the inner ear as noted above, cochlear implant electrode array – based DNA electrotransfer has been developed for *in vivo* applications. This platform, being developed out of UNSW Sydney under the trademark BaDGE® ('Bionic array Directed Gene Electrotransfer'), stems from modification of the cochlear implant electrode array, via parallel connection of gangs of electrodes, to create a highly focused electric field enabling close-field electroporation (Pinyon et al., 2014). This provides efficient gene electrotransfer at significantly lower voltages than that required for conventional electroporation. For example, in contrast to the high voltages required for open-field electroporation (above), Fig. 2C of

473
474
475 Pinyon et al., 2014 indicates thresholds of < 10 V applied to the cochlear implant array
476 electrodes wired in a ‘tandem’ configuration; the relationship of voltages, currents and charge
477 transfer used for close-field electroporation against achieved GFP reporter expression in the
478 guinea pig cochlea are evaluated in supplementary information Table S1 in that study. It is
479 significant that the GFP-positive mesenchymal cell counts at threshold, while inherently under-
480 sampling the actual number in decalcified whole-mounts of regions of the cochlea, are in the
481 tens of cells, and higher voltages achieve many hundreds of cells, which none-the-less represent
482 a more physiologically relevant mechanism for restoring focal neurotrophin expression to the
483 cochlea than the broad transduction inherent to viral vector-based gene delivery. The anatomy
484 of the cochlea also lends itself to this application, as perfusion of the perilymphatic space
485 achieves uniformity of the naked DNA concentration. For example, in initial *ex vivo* and *in*
486 *vivo* experiments in guinea pigs, buffered plasmid DNA solution was delivered via a tube
487 sealed to the perforated round window, flushing the perilymph out through the perforated oval
488 window membrane of scala vestibuli (via the apically-located helicotrema connection) (Pinyon
489 et al., 2014). Further refinement to include a lumen within the gene delivery array would enable
490 the DNA solution to leave from the tip and flow back along the array to exit via the round
491 window. The proof of concept experiments demonstrated take-up of plasmid DNA encoding
492 BDNF by the mesenchymal (mesothelial) cells lining the perilymphatic compartment of the
493 cochlea. In doing so, the production of recombinant neurotrophins by a relatively small group
494 of these mesenchymal cells was shown to stimulate outgrowth of the auditory nerve fibres
495 into close proximity with the cochlear implant electrodes, thereby closing the neural gap and
496 functionally improving the interface with the cochlear implant array as anticipated (Browne et
497 al., 2016; Housley et al., 2016; Pinyon et al., 2018; Pinyon et al., 2014).

512 With respect to the constrained geometry of the cochlear structure, the establishment of
513 electric fields for therapeutic DNA electrotransfer *in vivo* using conventional open-field
514 electroporation is impracticable, both with respect to electrode placement, and also the
515 associated high charge delivery in close proximity to the organ of Corti and spiral ganglion
516 (Fig. 1). A key factor for gene delivery to the cochlea is the consideration of the complex
517 compartmentalization and complex differentiation of the tissue within a very small overall
518 tissue volume, encased within the temporal bone. For example, in the guinea pig and humans,
519 the volume of the scala tympani, are just $4.8 \mu\text{l}$ and $29.2 \mu\text{l}$ respectively (Thorne et al., 1999).

525 Cochlear implant array – based DNA electrotransfer is based on control of the current
526 paths between multiple electrodes. Early experiments using *in situ* – *ex vivo* electrode array-
527 based DNA electrotransfer in guinea pig cochlea with DNA encoding fluorescent reporters
528
529
530
531

532
533
534 (Fig. 2A; Fig.3A) showed that the electrode configuration was a key determinant of the high
535 efficiency of this process. Neither use of pairs of adjacent platinum ring electrodes (~ 350 µm
536 diameter x 350 µm width), nor use of multiple electrodes in alternating anode and cathode
537 configuration, was as efficient as the ganged wiring of multiple adjacent electrodes in a linear
538 orientation, into distributed anodes and cathodes (designated ‘tandem’ configuration).
539 Subsequent *in vivo* guinea pig cochlea green fluorescent protein (GFP) reporter DNA
540 electrotransfer studies (Fig. 3B, Fig. 4) confirmed the efficacy of this tandem electrode
541 configuration (Browne et al., 2016; Pinyon et al., 2014) (Fig. 3B, C; Fig. 4).
542
543

544 Local production of BDNF by the mesenchymal cells was confirmed by
545 immunofluorescence detecting the FLAG-tag incorporated in the pShuttle-CMVp-BDNFflag-
546 IRES-GFPnls expression cassette (Fig. 5). *Ex vivo* experiments confirming the localized BDNF
547 production progressed to *in vivo* studies in an ototoxic deafened guinea pig, using an
548 intravenous (i.v.) furosemide and subcutaneous (s.c.) kanamycin treatment, followed by a two
549 week period that established hair cell loss and regression of the auditory nerve fibres within
550 the osseous spiral lamina model ((Pinyon et al., 2014); including supplementary material). The
551 cochlear implant array - based DNA electrotransfer BDNF gene augmentation treatment was
552 then provided unilaterally and strong nerve fibre regeneration was observed from around one
553 week post DNA delivery (Fig. 6). This re-growth of the auditory nerve fibres persisted for
554 several weeks beyond when episomal BDNF-encoding plasmid expression ceased (based on
555 detection of GFP fluorescence in the target mesenchymal cells lining scala tympani). A key
556 finding was that the regenerated neurites migrated through the osseous spiral lamina, or in some
557 cases, extended via the canaliculae perforantes (small pores) of the cochlear modiolar wall, to
558 end with discrete ectopic terminal sprouting within scala tympani. This was aided by the
559 scaffolding that was provided by the fibrosis that arises as an inflammatory response to the
560 cochlear implant array insertion. The local termination of the regenerated processes was ideal
561 in that no lateral extension of the afferents was apparent, and hence the tonotopic representation
562 of the radial fibres is likely to be maintained. These findings provide significant indicators of
563 safety and efficacy of cochlear implant array - based DNA electrotransfer. While the discrete
564 electrotransfer pulse train was at voltages that exceeded the charge transfer limits for the Pt
565 electrodes, such upper charge limits were established for continuous stimulation via cochlear
566 implants. Further, recent studies have shown that cochlear tissues are robust, even when higher
567 than normal charge transfers are delivered continuously via cochlear implants (Shepherd et al.,
568 2018). In the cochlear implant array - based DNA electrotransfer studies, there was no evident
569 tissue injury in the cochlea based on histology and the target mesenchymal cells were vital and
570
571
572
573
574
575
576
577
578
579
580
581
582
583
584
585
586
587
588
589
590

591
592
593 expressed the plasmid DNA gene cassettes to levels that were physiologically relevant with
594 respect to driving spiral ganglion nerve regeneration via production of BDNF, or indeed
595 expression of a range of reporter genes.
596
597

598 The functional efficacy of BDNF- cochlear implant array - based DNA electrotransfer
599 treatment to enhance the bionic interface was confirmed using electrically-evoked auditory
600 brainstem response (eABR) measurements in guinea-pigs with chronic cochlear implants,
601 using bipolar stimulation via the implant (Fig. 7). The differential between the significantly
602 lower eABR thresholds following the gene augmentation treatment and a control group where
603 a GFP reporter plasmid was maintained out to one month (Fig. 8) with sustained heightened
604 input-output functions reflecting greatly improved progressive neural recruitment (dynamic
605 range) (Pinyon et al., 2014). This proof of principle to enhance cochlear implant performance
606 paves the way for a regulatory permissive use of BaDGE® for cochlear therapeutics and in
607 particular, use of localized BDNF expression at low levels, to ‘close the neural gap’ with
608 cochlear implant arrays, which potentially could reduce current stimulation levels (reducing
609 power consumption) and improve the electrode placement discrimination (resulting in better
610 pitch perception). This is supported by the finding that lowered stimulus thresholds with
611 cochlear implant stimulation in deafened cats following neurotrophin treatment to regenerate
612 the auditory nerve fibres, was associated with narrowing of spatial tuning curves in the inferior
613 colliculus (Landry et al., 2013). The potential benefits of an enhanced neural interface for
614 cochlear implant systems will be assessed by translationally focused studies, and an initial
615 phase I/II clinical trial to evaluate the potential of this novel DNA therapeutics technology.
616
617
618
619
620
621
622
623
624
625
626

627 **2.3. Modelling array-based electric field focusing for naked DNA electrotransfer**

628
629 The underlying mechanism for the efficiency of bionic array directed gene
630 electrotransfer, has been established in GFP reporter plasmid DNA electrotransfer experiments
631 using adherent HEK293 cells on coverslips as the “target tissue”, overlaid by an eight node
632 cochlear implant array. Here it was shown that the tandem gene delivery array configuration
633 caused a substantial compression of the electric field centre around the null between the ganged
634 anodes and cathodes. As such, the absolute voltage in the solution in this zone was found to
635 be very low relative to other regions around the array, but the local voltage differential (change
636 in voltage over distance = electric field strength) was found to be equivalent to fields requiring
637 many hundreds of volts under conventional open-field electroporation where the tissue was
638 located between a pair of electrodes (Browne et al., 2016). This has been modelled (Fig. 9) and
639 the electric field map around the bionic array correlates closely with the bioreporter mapping
640
641
642
643
644
645
646
647
648
649

650
651
652 of the effective electric field for bionic array directed gene electrotransfer in the HEK293 cell
653 monolayers (Fig. 10). Array-based electric field focusing therefore enables local directed DNA
654 transfer into the cochlea using significantly lower charge delivery and hence is intrinsically
655 less likely to cause tissue damage. This principal is also evidently applicable to other
656 applications where DNA payload titration and localized targeting of DNA-based therapeutics
657 is advantageous.
658
659
660
661

662 Based on the efficiency of bionic array – based gene electrotransfer, and this modelling
663 of electric fields, the question arises as to whether contemporary cochlear implant devices may
664 have the intrinsic capability for naked DNA gene electrotransfer at charge transfer levels not
665 much greater than the current upper limits for cochlear implant devices. This does not seem
666 likely, given the rail voltage of cochlear implant devices is ~ 10 V to generate a maximum
667 constant current output of ~ 1 mA, limited to a few tens of μ s per pulse. Not only is the electric
668 field at , or below, the threshold for gene electrotransfer (~ 1 mV / μ m (Briaire et al., 2000)),
669 but it is evident from our evaluation of pulse duration, that at such low effective field strengths,
670 pulse durations of many tens of milliseconds is required for gene electrotransfer (Browne et
671 al., 2016), which is not possible using the inductive power transfer modality of cochlear
672 implants. Future generations of cochlear implants may well be designed to incorporate gene
673 electrotransfer modalities, depending upon the findings of the initial clinical trials which
674 require stand-alone systems using a dual array insertion protocol.
675
676
677
678
679
680
681
682

683 With regard to potential tissue injury from the electric pulses used for DNA
684 electrotransfer, conventional ‘open-field’ electroporation is known to produce both reversible
685 and none-reversible (cell death-causing) cell permeability. In addition, when voltages applied
686 to the electrodes exceed the Faradaic capacity, which for Pt/Ir electrodes occurs at voltages
687 above ~ 2.8V, then gassing occurs which affects pH and causes Cl₂ production, both of which
688 impact on cell viability. In the context of cochlear implant – based gene electrotransfer, this is
689 balanced against the fact that typically less than 10 electric monopolar electric pulses are used,
690 whereas the lower amplitude current pulses used for cochlear nerve stimulation by cochlear
691 implants are balanced but continuous and at kHz frequency. Clearly, the development of safe
692 gene electrotransfer into the cochlea will require studies that identify the minimal charge
693 transfer required to safely achieve consistent numbers of transfected mesenchymal cells to
694 produce physiologically relevant neurotrophin levels. This is evidently achievable based on the
695 lack of histopathology associated with the region of transduced mesenchymal cells in the
696 animal gene electrotransfer studies.
697
698
699
700
701
702
703
704
705
706
707
708

2.4. Extension of cochlear bionic array directed gene electrotransfer towards clinical trial

A key aspect of clinical translation of DNA electrotransfer-based therapeutics is the use of plasmids that lack antibiotic resistance genes (European_Medicines_Agency, 2008; European_Medicines_Agency, 2015; FDA, 1998; FDA, 2007). The rationale for this is that DNA electrotransfer could potentially drive expression of conventional plasmid DNA that incorporate antibiotic resistance selection genes in commensal bacteria within the surgical field. To this end, plasmids are being re-engineered to facilitate the translational pathway for this gene therapy modality. We are utilizing a pFAR4 plasmid (version 4 of a ‘plasmid Free of Antibiotic Resistance’) developed by co-authors Daniel Scherman and Corinne Marie at Descartes University, Paris. The pFAR4 plasmid backbone will also be used in a clinical trial for a gene electrotransfer-based treatment for macular degeneration (Thumann et al., 2017). As a pre-clinical workup to a bionic array directed gene electrotransfer - based cochlear neurotrophin gene therapy application, we undertook control studies using a GFP reporter expression cassette under a CMV promoter on the pFAR4 miniplasmid backbone. The pFAR4-CMVp-GFP DNA is significantly smaller than conventional plasmids (1130 bp backbone), as it omits the typical antibiotic resistance expression cassette, and selection is mediated by a (small) suppressor t-RNA motif that restores functional thymidylate synthase (ThyA) to a proprietary *Escherichia coli* cell line where *thyA* is mutated (Marie et al., 2010). The smaller size of pFAR4 is thought to improve gene transfer efficiency (Bloquel et al., 2004). These experiments confirmed the effectiveness of the pFAR4 plasmid for cochlear implant array directed gene electrotransfer (Fig. 11). Confocal imaging revealed the GFP reporter signal was confined to mesenchymal cells lining both scala tympani and scala vestibuli in the basal turn of the cochlea. This included prominent labelling of Reissner’s membrane, which is integral to the cochlear partition isolating scala media. There was no reporter expression in the three more apical turns, even though the reporter DNA solution was perfused throughout all four turns. This is indicative of the localized gene electrotransfer produced by the bionic array in a ‘tandem’ configuration of ganged anodes and cathodes. Thus, a key safety feature of bionic array directed DNA electrotransfer is that the biologically active zone for expression of the recombinant proteins is determined by the electric field focusing (electrode configuration and electric pulse parameters). The naked plasmid DNA outside of the electrotransfer zone (both scala tympani and scala vestibuli were perfused) is biologically inert and is subject to degradation by nucleases. For clinical trials, the pFAR4 plasmid backbone can be engineered to incorporate a humanized neurotrophin expression cassette. Delivery of the plasmid DNA could ideally be confined to scala tympani by pumping the DNA solution out of the tip of the

768
769
770 gene electrotransfer array via incorporation of a lumen through the core of the array. This would
771 enhance the targeting of neurotrophin production, and hence directional cues for spiral ganglion
772 neurite extension towards the subsequently inserted permanent cochlear implant array.
773
774
775
776

777 Based on these findings, bionic array directed gene electrotransfer is well positioned
778 for adoption as a means for neurotrophin gene augmentation during cochlear implant surgery.
779 In such a procedure, an otologist would temporarily insert a gene delivery array with integrated
780 delivery of neurotrophin-encoding DNA (BDNF and NT-3). The array would have the same
781 mechanical characteristics as the standard arrays used clinically, to avoid damaging the tissues.
782 Immediately after sufficient DNA solution has been injected from the tip of the array (to flow
783 back out through the perforated round window membrane, or cochleostomy), the gene
784 electrotransfer would be undertaken by passing electric pulses across the electrode array. Gene
785 electrotransfer has been shown to be effectively instantaneous (Escoffre et al., 2011), and in
786 the cochlear implant application, the gene delivery array could be removed immediately – as a
787 disposable item and the routine cochlear implant procedure would resume with implantation of
788 the device of choice. The expression of neurotrophins within hours of the procedure may well
789 enhance survival of the spiral ganglion neurons in the face of the trauma of the surgical
790 procedure (Bas et al., 2015). Peak expression of the BDNF plasmid DNA occurs within a few
791 days, promoting rapid regrowth of the spiral ganglion neurites within the osseous spiral lamina
792 and towards the neurotrophin-expressing mesenchymal cells, thereby reducing the neural-gap
793 with the bionic interface. The caveats to this are the unknowns related to the potential for spiral
794 ganglion neurite regeneration in human subjects who have had sensorineural hearing loss for
795 many years. Temporal bone studies have shown significant retention of spiral ganglion
796 neurons, particularly in the more apical regions of the cochlea, and given the success of
797 cochlear implant treatment in the elderly, this is clearly compatible with neurotrophin-based
798 auditory nerve regeneration strategies (Nadol, 1997). It is unclear whether the osseous spiral
799 lamina will support the outgrowth of the radial fibres in the manner seen with the preclinical
800 acute deafness induced in guinea pigs, but histological analysis of cochleae from elderly
801 subjects demonstrates surprising patency (Glueckert et al., 2005), and in addition, alternative
802 pathways for outgrowth of fibres towards the cochlear implant electrodes, such as via the
803 canaliculae perforantes (Shepherd et al., 2004) were evident in the bionic array directed gene
804 electrotransfer guinea pig cochlea studies (Pinyon et al., 2014).
805
806
807
808
809
810
811
812
813
814
815
816
817
818
819
820

821 Central to the safety and efficacy of gene therapy is regulation of expression. While
822 conditionally-regulated gene constructs are routine practice in animal models, such as the use
823
824
825
826

827
828
829 of tamoxifen to activate a Cre -estrogen receptor fusion protein (Metzger et al., 1995), such
830 switches are problematic for human trials, and considerable research development is on-going
831 around such platforms to support viral vector-based gene therapy applications (for example
832 “RheoSwitch Therapeutic system[®] / RTS[®]” (Barrett et al., 2018)). At one end of the spectrum,
833 in the case of an adverse reaction to the treatment, a mechanism for terminating the action is
834 highly desirable, while the ability to control the level of expression of the recombinant protein,
835 and limit action to the target site, are clear aspirations of the field. In the cochlear implant
836 neurotrophin gene augmentation application, control of BDNF in terms of location, level and
837 duration of expression therefore need to be considered. It is known that a range of neurotrophic
838 factors, including BDNF are upregulated in vestibular schwannomas (acoustic neuroma)
839 (Kramer et al., 2010) and likely promote metastatic progression. Clearly existence of such a
840 tumor would be an exclusion criteria for any future cochlear implant-associated neurotrophin
841 clinical trial. As noted above, over-expression of GDNF via AAV5 vector delivery to the
842 cochlea leads to off-target pathology in the CNS in a mouse model (Akil et al., 2018).
843
844
845
846
847
848
849
850
851

852 The expression profile of neurotrophins in the cochlea driven by bionic array directed
853 gene electrotransfer is likely to be influenced by the nature of the promoter and the plasmid
854 backbone, as well as the underlying fate of the target mesenchymal cells. This was explored in
855 a study that incorporated dual plasmid reporter expression (two plasmid DNAs delivered as 1:1
856 mix), both in the bionic array directed gene electrotransfer HEK293 cell monolayer model and
857 in the cochleae of normal hearing guinea-pigs (Pinyon et al., 2018). This study had a number
858 of key findings. Central to clinical translation, the fate of the transfected target cells was
859 followed by analysis of the ratio of red (mCherry):green (GFP) fluorescent reporter proteins
860 from the dual plasmid electrotransfer. In the HEK293 cell monolayer model, the ratio of
861 yellow-fluorescence (colocalized expression of red:green reporter coding plasmids) dropped
862 off across the days and weeks following the bionic array directed gene electrotransfer
863 procedure, which was directly related to cell division -based dilution of episomal expression
864 of the many tens of functional copies of the plasmids achieved by electrotransfer, while the
865 number of cells expressing either red or green fluorescence reporter proteins was sustained;
866 indicative of stable single-copy expression. However, in the guinea-pig cochlea bionic array
867 directed gene electrotransfer experiments, the ratios of red:green:yellow fluorescence of the
868 target perilymphatic compartment mesenchymal cells was stable at ~50%, but expression
869 declined to zero by the end of the three week monitoring period. This most likely reflects the
870 fact that mesenchymal cells are terminally differentiated and are turning over with time, with
871 replacement cells derived from precursor cells that were not transfected by bionic array directed
872
873
874
875
876
877
878
879
880
881
882
883
884
885

886
887
888
889 gene electrotransfer (Pinyon et al., 2018). This is also consistent with the observation in the
890 original experiments (Pinyon et al., 2014), where the limit of detection of GFP reporter
891 expression was ~ 6 weeks, with no detectable expression at 10 weeks. Therefore in this
892 application, recombinant neurotrophin expression is likely to be limited in the spatiotemporal
893 domains, with limited numbers of cells of finite duration, as distinct from the situation where
894 viral vectors drive sustained episomal expression in neurons, which have an indefinite lifespan.
896

897
898 In the context of the potential use of the pFAR4 miniplasmid for cochlear neurotrophin
899 gene augmentation, it is notable that while pFAR4 has been shown to provide sustained
900 expression in liver for more than six months, potentially attributable to the minimization of
901 bacterial DNA sequence which tends to induce gene silencing (Quiviger et al., 2014; Quiviger
902 et al., 2018), mesenchymal cell turnover is likely to be the key determining factor for
903 recombinant BDNF production. Given the limitations to gene expression with cochlear implant
904 array-based DNA electrotransfer as developed for neurotrophin gene augmentation, this raises
905 the question of whether the auditory nerve fibre regeneration is sustainable. The original study
906 (Pinyon et al., 2014) showed maintained functional improvement at one month - post DNA
907 electrotransfer in the deafened guinea pig model (see Fig. 8) and some myelinated fibres were
908 detectable within the basal turn scala tympani region out to ten weeks, albeit in a highly
909 diminished density compared with two to three weeks post-electrotransfer. It is anticipated that
910 in clinical applications, or pre-clinical models such as the deafened cat, where electrical
911 stimulation is provided to the regenerated nerve fibres by chronic use of the cochlear implant,
912 trophic action of the electrical stimulation may sustain the improved neural interface. There is
913 strong experimental evidence for this, based on deafened guinea pig and deafened cat studies
914 where auditory nerve fibre regeneration has been driven by BDNF treatment and spiral
915 ganglion neuron survival and nerve fibre density has been shown to be maintained after
916 cessation of BDNF when electrical stimulation by the cochlear implant is enabled (Landry et
917 al., 2013; Leake et al., 2013; Pettingill et al., 2011; Shepherd et al., 2008). Thus temporary
918 cessation of use of the cochlear implant offers a means to 'reset' the spiral ganglion neuron
919 phenotype, should the neurotrophin gene therapy produce an unanticipated adverse effect on
920 hearing performance, such as a reduction in CNC word scores over time, where an
921 improvement is typical.
922
923
924
925
926
927
928
929
930
931
932
933
934
935

936 The progression to clinical trials for bionic array directed gene electrotransfer - based
937 neurotrophin gene augmentation in the cochlea would broadly advance directed gene delivery
938 technology, provide new knowledge on the effects of recombinant neurotrophins in the inner
939 ear, and establish the multi-disciplinary expertise and regulatory pathway framework needed
940
941
942
943
944

945
946
947 to broadly advance gene-based inner ear therapeutics. If the clinical outcomes of such trials
948 approach the speculated potential, cochlear gene augmentation therapy may become a standard
949 treatment practice to achieve optimum hearing with cochlear implants, particularly for patients
950 with severe - profound sensorineural hearing loss.
951
952
953
954
955

956 **Funding**

957 Supported by funding from the Australian Research Council (ARC), grants (ARC
958 DP151014754, ARC LP0992098, ARC LP140101008), the Garnett Passe and Rodney
959 Williams Memorial Foundation, and the National Health and Medical Research Council
960 (NHMRC) grants APP1091646, APP1122055 and GNT1142910. The research was supported
961 by collaborative research funding from Cochlear Ltd.
962
963
964
965
966
967

968 **Declaration of interest**

969 The BaDGE[®] registered trademark is assigned to UNSW Sydney Knowledge Exchange
970 though New South Innovations Pty Ltd, which is also the assignee for the BaDGE[®]-related
971 intellectual property.
972
973
974
975
976
977
978
979
980
981
982
983
984
985
986
987
988
989
990
991
992
993
994
995
996
997
998
999
1000
1001
1002
1003

References

- Akil, O., Blits, B., Lustig, L.R., Leake, P.A. 2018. Virally Mediated Overexpression of Glial-Derived Neurotrophic Factor Elicits Age- and Dose-Dependent Neuronal Toxicity and Hearing Loss. *Hum Gene Ther*.
- Akil, O., Seal, R.P., Burke, K., Wang, C., Alemi, A., During, M., Edwards, R.H., Lustig, L.R. 2012. Restoration of hearing in the VGLUT3 knockout mouse using virally mediated gene therapy. *Neuron* 75, 283-93.
- Baker, K., Brough, D.E., Staecker, H. 2009. Repair of the vestibular system via adenovector delivery of *Atoh1*: a potential treatment for balance disorders. *Adv Otorhinolaryngol* 66, 52-63.
- Barrett, J.A., Cai, H., Miao, J., Khare, P.D., Gonzalez, P., Dalsing-Hernandez, J., Sharma, G., Chan, T., Cooper, L.J.N., Lebel, F. 2018. Regulated intratumoral expression of IL-12 using a RheoSwitch Therapeutic System((R)) (RTS((R))) gene switch as gene therapy for the treatment of glioma. *Cancer Gene Ther* 25, 106-116.
- Bas, E., Goncalves, S., Adams, M., Dinh, C.T., Bas, J.M., Van De Water, T.R., Eshraghi, A.A. 2015. Spiral ganglion cells and macrophages initiate neuro-inflammation and scarring following cochlear implantation. *Front Cell Neurosci* 9, 303.
- Belyantseva, I.A. 2009. Helios Gene Gun-mediated transfection of the inner ear sensory epithelium. *Methods Mol Biol* 493, 103-23.
- Bloquel, C., Fabre, E., Bureau, M.F., Scherman, D. 2004. Plasmid DNA electrotransfer for intracellular and secreted proteins expression: new methodological developments and applications. *J Gene Med* 6 Suppl 1, S11-23.
- Briaire, J.J., Frijns, J.H. 2000. Field patterns in a 3D tapered spiral model of the electrically stimulated cochlea. *Hear Res* 148, 18-30.
- Brough, D.E., ETTYREDDY, D.R. 2016. Adenoviral vector encoding human atonal homolog-1 (HATH1). In: Organization, W.I.P., (Ed.). Genvec, Inc.
- Browne, C.J., Pinyon, J.L., Housley, D.M., Crawford, E.N., Lovell, N.H., Klugmann, M., Housley, G.D. 2016. Mapping of bionic array electric field focusing in plasmid DNA-based gene electrotransfer. *Gene Ther* 23, 369-79.
- Budenz, C.L., Pflingst, B.E., Raphael, Y. 2012. The use of neurotrophin therapy in the inner ear to augment cochlear implantation outcomes. *Anat Rec (Hoboken)* 295, 1896-908.
- Driver, E.C., Kelley, M.W. 2010. Transfection of mouse cochlear explants by electroporation. *Curr Protoc Neurosci Chapter 4, Unit 4 34* 1-10.
- Escoffre, J.M., Portet, T., Favard, C., Teissie, J., Dean, D.S., Rols, M.P. 2011. Electromediated formation of DNA complexes with cell membranes and its consequences for gene delivery. *Biochim Biophys Acta* 1808, 1538-43.
- European_Medicines_Agency. 2008. Guideline on the non-clinical studies required before first clinical use of gene therapy medicinal products. EMEA/CHMP/GTWP/125459/2006, 10.
- European_Medicines_Agency. 2015. Guideline on the quality, non-clinical and clinical aspects 4 of gene therapy medicinal products. EMA/CAT/80183/2014, 42.
- FDA. 1998. Guidance for Industry: Guidance for Human Somatic Cell and Gene Therapy.
- FDA. 2007. Guidance for Industry: Considerations for plasmid DNA Vaccines for Infectious Disease.
- Fransson, A., Ulfendahl, M. 2017. Structural changes in the inner ear over time studied in the experimentally deafened guinea pig. *J Neurosci Res* 95, 869-875.

- 1063
1064
1065
1066
1067
1068
1069
1070
1071
1072
1073
1074
1075
1076
1077
1078
1079
1080
1081
1082
1083
1084
1085
1086
1087
1088
1089
1090
1091
1092
1093
1094
1095
1096
1097
1098
1099
1100
1101
1102
1103
1104
1105
1106
1107
1108
1109
1110
1111
1112
1113
1114
1115
1116
1117
1118
1119
1120
1121
- Fransson, A., Tornøe, J., Wahlberg, L.U., Ulfendahl, M. 2018. The feasibility of an encapsulated cell approach in an animal deafness model. *J Control Release* 270, 275-281.
- Glueckert, R., Pfaller, K., Kinnefors, A., Rask-Andersen, H., Schrott-Fischer, A. 2005. The human spiral ganglion: new insights into ultrastructure, survival rate and implications for cochlear implants. *Audiol Neurootol* 10, 258-73.
- Hendricks, J.L., Chikar, J.A., Crumling, M.A., Raphael, Y., Martin, D.C. 2008. Localized cell and drug delivery for auditory prostheses. *Hear Res* 242, 117-31.
- Housley, G.D., Browne, C.J., Crawford, E.N., Klugmann, M., Lovell, N.H., Pinyon, J.L. 2016. Cochlear Implant Close-Field Electroporation. In: Miklavčič, D., (Ed.), *Handbook of Electroporation*. Springer. pp. 1-20. DOI 10.1007/978-3-319-26779-1_59-1.
- Husseman, J., Raphael, Y. 2009. Gene therapy in the inner ear using adenovirus vectors. *Adv Otorhinolaryngol* 66, 37-51.
- Izumikawa, M., Minoda, R., Kawamoto, K., Abrashkin, K.A., Swiderski, D.L., Dolan, D.F., Brough, D.E., Raphael, Y. 2005. Auditory hair cell replacement and hearing improvement by *Atoh1* gene therapy in deaf mammals. *Nat Med* 11, 271-6.
- Kamakura, T., Nadol, J.B., Jr. 2016. Correlation between word recognition score and intracochlear new bone and fibrous tissue after cochlear implantation in the human. *Hear Res* 339, 132-41.
- Kawamoto, K., Ishimoto, S., Minoda, R., Brough, D.E., Raphael, Y. 2003. *Math1* gene transfer generates new cochlear hair cells in mature guinea pigs in vivo. *J Neurosci* 23, 4395-400.
- Kelley, M.W. 1997. Cellular commitment and differentiation in the cochlea: potential advances using gene transfer. *Audiol Neurootol* 2, 50-60.
- Kramer, F., Stover, T., Warnecke, A., Diensthuber, M., Lenarz, T., Wissel, K. 2010. BDNF mRNA expression is significantly upregulated in vestibular schwannomas and correlates with proliferative activity. *J Neurooncol* 98, 31-9.
- Lacković, I., Magjarević, R., D., M. 2009. Three-dimensional finite-element analysis of joule heating in electrochemotherapy and in vivo gene electrotransfer. *IEEE Transactions on Dielectrics and Electrical Insulation* 16, 1338 - 1347.
- Landegger, L.D., Pan, B., Askew, C., Wassmer, S.J., Gluck, S.D., Galvin, A., Taylor, R., Forge, A., Stankovic, K.M., Holt, J.R., Vandenbergh, L.H. 2017. A synthetic AAV vector enables safe and efficient gene transfer to the mammalian inner ear. *Nat Biotechnol* 35, 280-284.
- Landry, T.G., Fallon, J.B., Wise, A.K., Shepherd, R.K. 2013. Chronic neurotrophin delivery promotes ectopic neurite growth from the spiral ganglion of deafened cochleae without compromising the spatial selectivity of cochlear implants. *The Journal of comparative neurology*.
- Leake, P.A., Hradek, G.T., Rebscher, S.J., Snyder, R.L. 1991. Chronic intracochlear electrical stimulation induces selective survival of spiral ganglion neurons in neonatally deafened cats. *Hear Res* 54, 251-71.
- Leake, P.A., Stakhovskaya, O., Hetherington, A., Rebscher, S.J., Bonham, B. 2013. Effects of brain-derived neurotrophic factor (BDNF) and electrical stimulation on survival and function of cochlear spiral ganglion neurons in deafened, developing cats. *J Assoc Res Otolaryngol* 14, 187-211.
- Li, Y., Jia, Y.C., Cui, K., Li, N., Zheng, Z.Y., Wang, Y.Z., Yuan, X.B. 2005. Essential role of TRPC channels in the guidance of nerve growth cones by brain-derived neurotrophic factor. *Nature* 434, 894-8.
- Lustig, L.R., Akil, O. 2012. Cochlear gene therapy. *Curr Opin Neurol* 25, 57-60.

- 1122
1123
1124 Marie, C., Vandermeulen, G., Quiviger, M., Richard, M., Preat, V., Scherman, D. 2010.
1125 pFARs, plasmids free of antibiotic resistance markers, display high-level transgene
1126 expression in muscle, skin and tumour cells. *J Gene Med* 12, 323-32.
1127
1128 Metzger, D., Clifford, J., Chiba, H., Chambon, P. 1995. Conditional site-specific
1129 recombination in mammalian cells using a ligand-dependent chimeric Cre
1130 recombinase. *Proceedings of the National Academy of Sciences of the United States*
1131 *of America* 92, 6991-5.
1132
1133 Miller, J.M., Le Prell, C.G., Prieskorn, D.M., Wys, N.L., Altschuler, R.A. 2007. Delayed
1134 neurotrophin treatment following deafness rescues spiral ganglion cells from death
1135 and promotes regrowth of auditory nerve peripheral processes: effects of brain-
1136 derived neurotrophic factor and fibroblast growth factor. *J Neurosci Res* 85, 1959-69.
1137
1138 Nadol, J.B., Jr. 1997. Patterns of neural degeneration in the human cochlea and auditory
1139 nerve: implications for cochlear implantation. *Otolaryngol Head Neck Surg* 117, 220-
1140 8.
1141
1142 Nadol, J.B., Jr., Shiao, J.Y., Burgess, B.J., Ketten, D.R., Eddington, D.K., Gantz, B.J., Kos,
1143 I., Montandon, P., Coker, N.J., Roland, J.T., Jr., Shallop, J.K. 2001. Histopathology of
1144 cochlear implants in humans. *Ann Otol Rhinol Laryngol* 110, 883-91.
1145
1146 Pan, B., Geleoc, G.S., Asai, Y., Horwitz, G.C., Kurima, K., Ishikawa, K., Kawashima, Y.,
1147 Griffith, A.J., Holt, J.R. 2013. TMC1 and TMC2 are components of the
1148 mechanotransduction channel in hair cells of the mammalian inner ear. *Neuron* 79,
1149 504-15.
1150
1151 Pan, B., Askew, C., Galvin, A., Heman-Ackah, S., Asai, Y., Indzhykulian, A.A., Jodelka,
1152 F.M., Hastings, M.L., Lentz, J.J., Vandenberghe, L.H., Holt, J.R., Geleoc, G.S. 2017.
1153 Gene therapy restores auditory and vestibular function in a mouse model of Usher
1154 syndrome type 1c. *Nat Biotechnol* 35, 264-272.
1155
1156 Pettingill, L.N., Wise, A.K., Geaney, M.S., Shepherd, R.K. 2011. Enhanced auditory neuron
1157 survival following cell-based BDNF treatment in the deaf guinea pig. *PLoS One* 6,
1158 e18733.
1159
1160 Phan, P.A., Tadros, S.F., Kim, Y., Birnbaumer, L., Housley, G.D. 2010. Developmental
1161 regulation of TRPC3 ion channel expression in the mouse cochlea. *Histochem Cell*
1162 *Biol* 133, 437-48.
1163
1164 Pharmaceuticals, N. 2019. Safety, Tolerability and Efficacy for CGF166 in Patients With
1165 Unilateral or Bilateral Severe-to-profound Hearing Loss.
1166 <https://clinicaltrials.gov/ct2/show/NCT02132130>.
1167
1168 Pinyon, J.L., Klugmann, M., Lovell, N.H., Housley, G.D. 2018. Dual-Plasmid Bionic Array-
1169 Directed Gene Electrotransfer in HEK293 Cells and Cochlear Mesenchymal Cells
1170 Probes Transgene Expression and Cell Fate. *Hum Gene Ther*.
1171
1172 Pinyon, J.L., Tadros, S.F., Froud, K.E., AC, Y.W., Tompson, I.T., Crawford, E.N., Ko, M.,
1173 Morris, R., Klugmann, M., Housley, G.D. 2014. Close-field electroporation gene
1174 delivery using the cochlear implant electrode array enhances the bionic ear
1175 (supplementary information). *Science Translational Medicine* 6 (233), 233ra54. [doi:
1176 10.1126/scitranslmed.3008177].
1177
1178 Praetorius, M., Hsu, C., Baker, K., Brough, D.E., Plinkert, P., Staecker, H. 2010.
1179 Adenovector-mediated hair cell regeneration is affected by promoter type. *Acta*
1180 *Otolaryngol* 130, 215-22.

- 1181
1182
1183
1184 Quiviger, M., Giannakopoulos, A., Verhenne, S., Marie, C., Stavrou, E.F., Vanhoorelbeke,
1185 K., Izsvak, Z., De Meyer, S.F., Athanassiadou, A., Scherman, D. 2018. Improved
1186 molecular platform for the gene therapy of rare diseases by liver protein secretion. *Eur*
1187 *J Med Genet* 61, 723-728.
- 1188 Ramekers, D., Versnel, H., Grolman, W., Klis, S.F. 2012. Neurotrophins and their role in the
1189 cochlea. *Hear Res* 288, 19-33.
- 1190 Rosazza, C., Meglic, S.H., Zumbusch, A., Rols, M.P., Miklavcic, D. 2016a. Gene
1191 Electrotransfer: A Mechanistic Perspective. *Curr Gene Ther* 16, 98-129.
- 1192 Rosazza, C., Deschout, H., Buntz, A., Braeckmans, K., Rols, M.P., Zumbusch, A. 2016b.
1193 Endocytosis and Endosomal Trafficking of DNA After Gene Electrotransfer In Vitro.
1194 *Mol Ther Nucleic Acids* 5, e286.
- 1195 Schlecker, C., Praetorius, M., Brough, D.E., Presler, R.G., Jr., Hsu, C., Plinkert, P.K.,
1196 Staecker, H. 2011. Selective atonal gene delivery improves balance function in a
1197 mouse model of vestibular disease. *Gene Ther* 18, 884-90.
- 1198 Seyyedi, M., Viana, L.M., Nadol, J.B., Jr. 2014. Within-subject comparison of word
1199 recognition and spiral ganglion cell count in bilateral cochlear implant recipients. *Otol*
1200 *Neurotol* 35, 1446-50.
- 1201 Shepherd, R.K., Colreavy, M.P. 2004. Surface microstructure of the perilymphatic space:
1202 implications for cochlear implants and cell- or drug-based therapies. *Arch*
1203 *Otolaryngol Head Neck Surg* 130, 518-23.
- 1204 Shepherd, R.K., Wise, A.K. 2014. Gene therapy boosts the bionic ear. *Sci Transl Med* 6,
1205 233fs17.
- 1206 Shepherd, R.K., Coco, A., Epp, S.B. 2008. Neurotrophins and electrical stimulation for
1207 protection and repair of spiral ganglion neurons following sensorineural hearing loss.
1208 *Hear Res* 242, 100-9.
- 1209 Shepherd, R.K., Carter, P.M., Enke, Y.L., Wise, A.K., Fallon, J.B. 2018. Chronic
1210 intracochlear electrical stimulation at high charge densities results in platinum
1211 dissolution but not neural loss or functional changes in vivo. *J Neural Eng* 16,
1212 026009.
- 1213 Shibata, S.B., Cortez, S.R., Beyer, L.A., Wiler, J.A., Di Polo, A., Pfungst, B.E., Raphael, Y.
1214 2010. Transgenic BDNF induces nerve fiber regrowth into the auditory epithelium in
1215 deaf cochleae. *Exp Neurol* 223, 464-72.
- 1216 Tadros, S.F., Kim, Y., Phan, P.A., Birnbaumer, L., Housley, G.D. 2010. TRPC3 ion channel
1217 subunit immunolocalization in the cochlea. *Histochem Cell Biol* 133, 137-47.
- 1218 Thorne, M., Salt, A.N., DeMott, J.E., Henson, M.M., Henson, O.W., Jr., Gewalt, S.L. 1999.
1219 Cochlear fluid space dimensions for six species derived from reconstructions of three-
1220 dimensional magnetic resonance images. *Laryngoscope* 109, 1661-8.
- 1221 Thumann, G., Harmening, N., Prat-Souteyrand, C., Marie, C., Pastor, M., Sebe, A., Miskey,
1222 C., Hurst, L.D., Diarra, S., Kropp, M., Walter, P., Scherman, D., Ivics, Z., Izsvak, Z.,
1223 Johnen, S. 2017. Engineering of PEDF-Expressing Primary Pigment Epithelial Cells
1224 by the SB Transposon System Delivered by pFAR4 Plasmids. *Mol Ther Nucleic*
1225 *Acids* 6, 302-314.
- 1226 Wang, L., Jiang, H., Brigande, J.V. 2012. Gene transfer to the developing mouse inner ear by
1227 in vivo electroporation. *J Vis Exp*.
- 1228 Wise, A.K., Richardson, R., Hardman, J., Clark, G., O'Leary, S. 2005. Resprouting and
1229 survival of guinea pig cochlear neurons in response to the administration of the
1230 neurotrophins brain-derived neurotrophic factor and neurotrophin-3. *The Journal of*
1231 *comparative neurology* 487, 147-65.
- 1232
1233
1234
1235
1236
1237
1238
1239

1240
1241
1242
1243 Wise, A.K., Tan, J., Wang, Y., Caruso, F., Shepherd, R.K. 2016. Improved Auditory Nerve
1244 Survival with Nanoengineered Supraparticles for Neurotrophin Delivery into the
1245 Deafened Cochlea. PLoS One 11, e0164867.
1246 Wise, A.K., Fallon, J.B., Neil, A.J., Pettingill, L.N., Geaney, M.S., Skinner, S.J., Shepherd,
1247 R.K. 2011. Combining cell-based therapies and neural prostheses to promote neural
1248 survival. Neurotherapeutics 8, 774-87.
1249 Wise, A.K., Hume, C.R., Flynn, B.O., Jeelall, Y.S., Suhr, C.L., Sgro, B.E., O'Leary, S.J.,
1250 Shepherd, R.K., Richardson, R.T. 2010. Effects of localized neurotrophin gene
1251 expression on spiral ganglion neuron resprouting in the deafened cochlea. Mol Ther
1252 18, 1111-22.
1253 Wong, S.P., Argyros, O., Harbottle, R.P. 2015. Sustained expression from DNA vectors. Adv
1254 Genet 89, 113-52.
1255 Xiong, W., Wagner, T., Yan, L., Grillet, N., Muller, U. 2014. Using injectoporation to deliver
1256 genes to mechanosensory hair cells. Nat Protoc 9, 2438-49.
1257 Zhao, H., Avenarius, M.R., Gillespie, P.G. 2012. Improved biolistic transfection of hair cells.
1258 PLoS One 7, e46765.
1259
1260
1261
1262
1263
1264
1265
1266
1267
1268
1269
1270
1271
1272
1273
1274
1275
1276
1277
1278
1279
1280
1281
1282
1283
1284
1285
1286
1287
1288
1289
1290
1291
1292
1293
1294
1295
1296
1297
1298

1299
1300
1301 **Figure Legends**
1302
1303

1304 **Fig. 1: Anatomy of the cochlea.** **A)** 3D reconstruction of confocal scans showing the 4
1305 spiraling turns of a hemi-sectioned guinea pig cochlea. The endolymph-filled compartment
1306 scala media (SM) is situated between the perilymphatic compartments scala tympani (ST) and
1307 scala vestibuli (SV), which meet at the apical helicotrema (H). Reissner's membrane (RM)
1308 separates scala media from scala vestibuli, with epithelial cells lining the endolymphatic
1309 surface and mesenchymal cells lining the perilymphatic surface. The sound-transducing
1310 sensory epithelium (SE) located between scala tympani and scala media is innervated by the
1311 spiral ganglion neurons. The cell bodies of these neurons are shown as yellow within
1312 Rosenthal's canal (RC). Green labelling is a neuronal-specific antibody (anti- β III tubulin)
1313 excited by a 488 nm argon ion laser, red is non-specific tissue autofluorescence excited by a
1314 561 nm diode pumped solid state laser, showing anatomical structure. **B)** A single confocal
1315 scan showing a close-up view of the sensory epithelium sitting on the basilar membrane (BM).
1316 Most of the green spiral ganglion neuron peripheral neurites innervate individual inner hair
1317 cells (IHC), with a subset innervating multiple outer hair cells (OHC) within the outer three
1318 rows. Blue signal shows the nuclear-specific DAPI stain and red shows a 647 nm-conjugated
1319 phalloidin, which specifically binds to the F-actin within stereocilia and cuticular plate regions
1320 of the hair cells and the pillar cells. Transmitted light resolving other structure is shown in grey.
1321
1322
1323
1324
1325
1326
1327
1328
1329
1330
1331
1332

1333 **Fig. 2: The guinea pig cochlear implant array-based DNA electrotransfer model.** **A)** Image
1334 of an isolated and decalcified guinea pig cochlea with an eight-electrode animal model cochlear
1335 implant array partially inserted (five of eight electrodes inside). When the cochlea is
1336 decalcified, as used in this demonstration, it becomes semi-transparent and thus three of the
1337 internal electrodes can be seen behind the outer capsule wall of basal scala tympani. **B)** Micro-
1338 CT generated image showing cochlear implant in situ within the skull of a chronically
1339 implanted guinea pig. Arrow indicates insertion of the 8 electrode array into the basal turn of
1340 the left cochlea.
1341
1342
1343
1344
1345
1346
1347

1348 **Fig. 3: Directed gene electrotransfer using the cochlear implant.** Epifluorescence images
1349 of resected guinea pig cochleae after array-based electrotransfer using a bicistronic plasmid
1350 encoding a nuclear localised GFP reporter along with a BDNF - encoding gene sequence driven
1351 by the cytomegalovirus promoter (pShuttle-CMVp-BDNFflag-IRES-GFPnls, after (Pinyon et
1352 al., 2014)). The bony outer capsule has been removed, with internal structure mostly still intact.
1353
1354
1355
1356
1357

1358
1359
1360 Bright white spots represent GFP positive transfected cells emitting green light after excitation
1361 with blue light. These cells are located in the basal of the four turns of the cochlea, in close
1362 proximity to the electrode array, which could only penetrate that region of scala tympani. **A)**
1363 GP296 - cochlear implant array-based DNA electrotransfer was performed ex vivo and the
1364 whole cochlea explant was cultured for 3 days ('alternating' electrode polarity configuration;
1365 20 x 50 ms pulses of 40 V at 1 Hz.). **B)** GP286 - - cochlear implant array-based DNA
1366 electrotransfer was performed in vivo using the same electrotransfer parameters as in (A), with
1367 the gene delivery array removed immediately after DNA electrotransfer and the tissue collected
1368 3 days later. **C)** GP293 – in vivo - cochlear implant array-based DNA electrotransfer as for (B),
1369 where the tissue was collected 2 days after gene delivery, showing the localisation of the GFP+
1370 cells in the basal turn, where the gene delivery array was inserted, despite the perfusion of the
1371 entire perilymphatic space with the reporter plasmid DNA. Unpubl. images (Pinyon et al.,
1372 2014).
1373
1374
1375
1376
1377
1378
1379
1380

1381
1382
1383 **Fig. 4: Three-dimensional confocal reconstruction of a guinea pig cochlea transfected**
1384 **with a plasmid DNA encoding a nuclear localized green fluorescent protein reporter via**
1385 **cochlear implant array-based DNA electrotransfer.** GFP+ cells are located on the basal
1386 modiolar wall, the cochlear structure imaged via background autofluorescence is shown in red.
1387 (GP276 tandem electrode array configuration, 40 V x 5 pulses x 50 ms at 1 Hz, 14 days after
1388 in vivo DNA electrotransfer, with the gene delivery array removed immediately). Plasmid:
1389 pShuttle-CMVp-BDNFflag-IRES-GFPnls. Unpubl. images (Pinyon et al., 2014).
1390
1391
1392
1393
1394

1395
1396 **Fig. 5: Production of recombinant brain-derived neurotrophic factor (BDNF) after gene**
1397 **electrotransfer using the cochlear implant.** Confocal 3D reconstructions of transfected cells
1398 expressing the nuclear localised GFP reporter gene (green) fluorescence and BDNF (red). The
1399 red signal represents a 594 nm conjugated antibody after anti-FLAG immunohistochemistry
1400 targeted at the FLAG-tagged recombinant BDNF encoded on the delivered plasmid DNA. **A)**
1401 A high magnification view of two cells located on the modiolar wall of basal scala tympani.
1402 GP-FB029 tandem 20 V x 5 pulses x 50 ms at 1 Hz, five days following DNA electrotransfer,
1403 with the gene delivery probe removed immediately. **B)** BDNF expressing cells on Reissner's
1404 membrane in the cochlea basal turn. GP-FB007 alternating 40 V x 20 pulses x 50 ms at 1 Hz,
1405 two days post ex vivo cochlear implant array-based DNA electrotransfer. Plasmid: pShuttle-
1406 CMVp-BDNFflag-IRES-GFPnls. Unpubl. images (Pinyon et al., 2014).
1407
1408
1409
1410
1411
1412
1413
1414
1415
1416

1417
1418
1419 **Fig. 6: Neurotrophin-induced cochlear nerve regeneration after Bionic Array Directed**
1420 **Gene Electrotransfer (BADGE)**. Confocal scans showing 50 μ m cryosections of cochleae
1421 from the left and right sides of deafened guinea pigs where the left cochleae received BADGE
1422 of the neurotrophin cassette 2 weeks after deafening (alternating configuration 40 V x 20 pulses
1423 x 50 ms at 1 Hz). **A)** Left treated cochlea of GP283 showing regeneration of the peripheral
1424 neurites of the spiral ganglion neurons in green. **B)** Right untreated cochlea from the same
1425 animal shown in (A). **C)** A second example of a left treated cochlea from another animal -
1426 GP284. **D)** The right control untreated cochlea from the animal in (C). **E)** A second 50 μ m
1427 cryosection from the left treated cochlea (GP284) also shown in (C). **F)** A high magnification
1428 image of the neurite outgrowth towards the flattened sensory epithelium shown in (E). Arrows
1429 point to the regenerated fibres throughout the fibre tracks in the osseous spiral lamina and
1430 ectopic branching into both scala tympani (ST) and scala media (SM). Green is neural specific
1431 staining (TUJ1) highlighting the nerve cell bodies and fibres. Red is autofluorescence of the
1432 bony tissue. Grey represents transmitted light showing cochlear structure. SV; scala vestibuli.
1433 Plasmid: pShuttle-CMVp-BDNFflag-IRES-GFPnls. Unpubl. images (Pinyon et al., 2014).
1434
1435
1436
1437
1438
1439
1440
1441
1442
1443
1444

1445 **Fig. 7: Enhanced cochlear implant performance after neurotrophin gene**
1446 **electrotransfer.** **A)** Acoustically-evoked auditory brainstem responses (ABRs) representative
1447 of those in normal hearing guinea pigs, prior to ototoxic treatment, in response to broadband
1448 click stimulus (dBSPL). **B)** Traces from the same animal in (A) recorded one-week after
1449 ototoxic treatment. No response was detected up to the maximum tested 90 dB SPL (85 dB
1450 and 90 dB traces not shown). **C)** Electrically-evoked auditory brainstem responses (eABRs)
1451 in a guinea pig 4 weeks after deafening and 2 weeks post cochlear implantation without
1452 neurotrophin gene therapy. **D)** eABRs in a guinea pig 4 weeks after deafening and 2 weeks
1453 post cochlear implantation and neurotrophin gene electrotransfer, showing recovery of neural
1454 integrity through reduced thresholds and increased magnitudes of recruitment. eABR used
1455 bipolar stimulation between ganged electrodes 1-4 and 5-8, corresponding to the ‘tandem’
1456 configuration; alternating monophasic constant current pulses of 100 μ s duration (averaged
1457 over 512 trials). Neurotrophin gene delivery utilised bionic array -based electrotransfer.
1458 Plasmid: pShuttle-CMVp-BDNFflag-IRES-GFPnls. Unpubl. images (Pinyon et al., 2014).
1459
1460
1461
1462
1463
1464
1465
1466
1467
1468

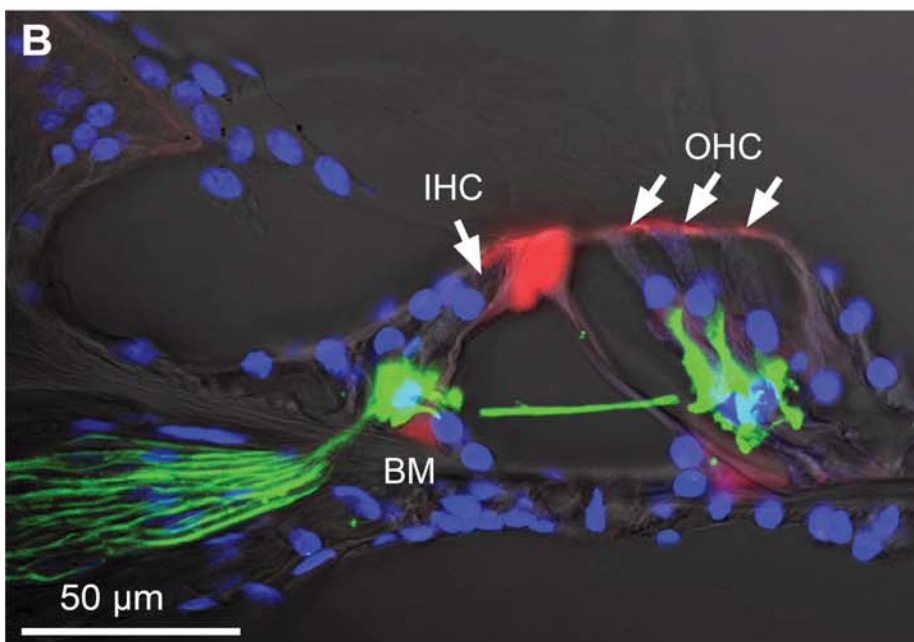
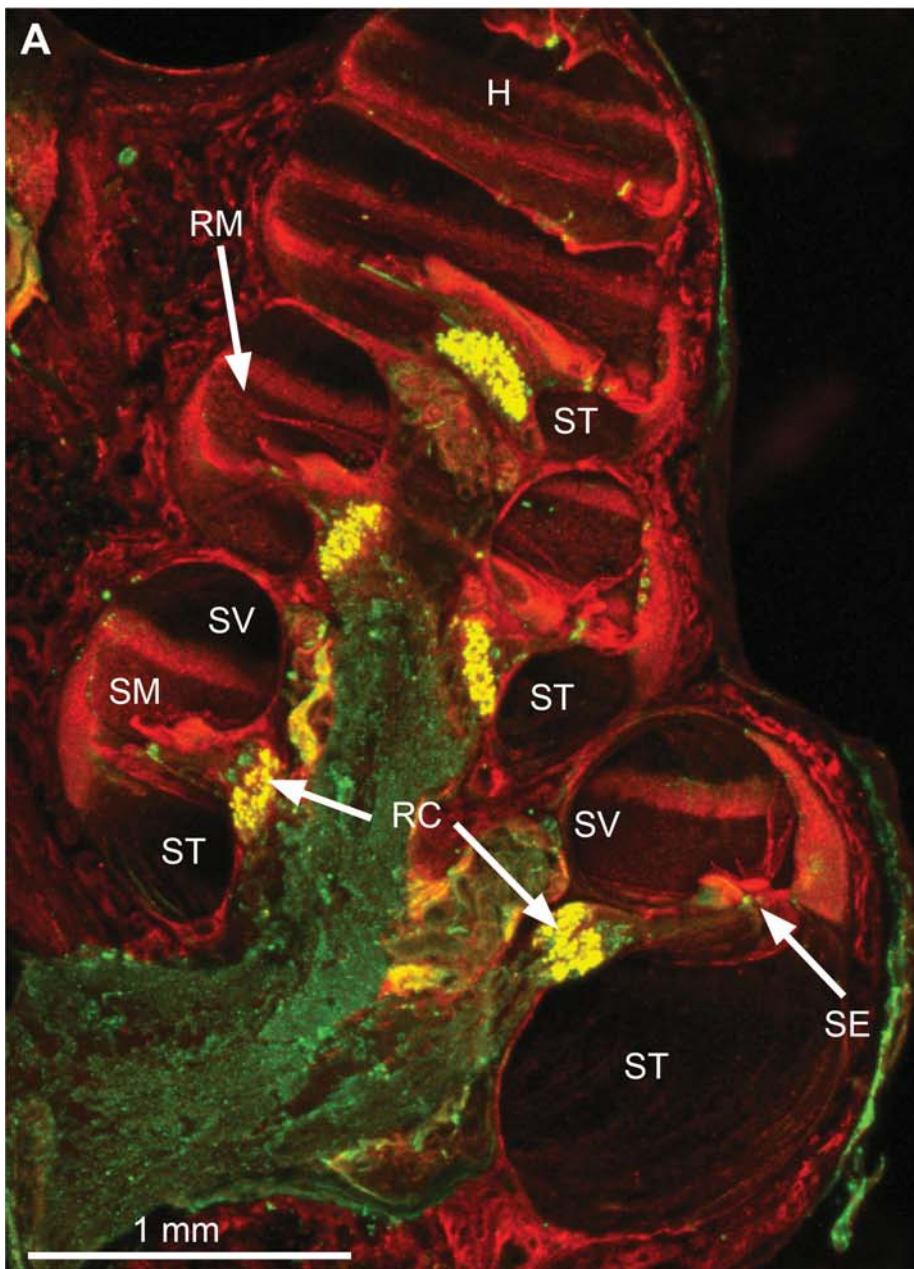
1469 **Fig. 8: Lowered eABR thresholds in guinea-pig cochleae treated with a BDNF-encoding**
1470 **plasmid via cochlear implant array - based DNA electrotransfer measured one month**
1471 **after electrotransfer.** These data show the maintenance of the improved bionic ear neural
1472
1473
1474
1475

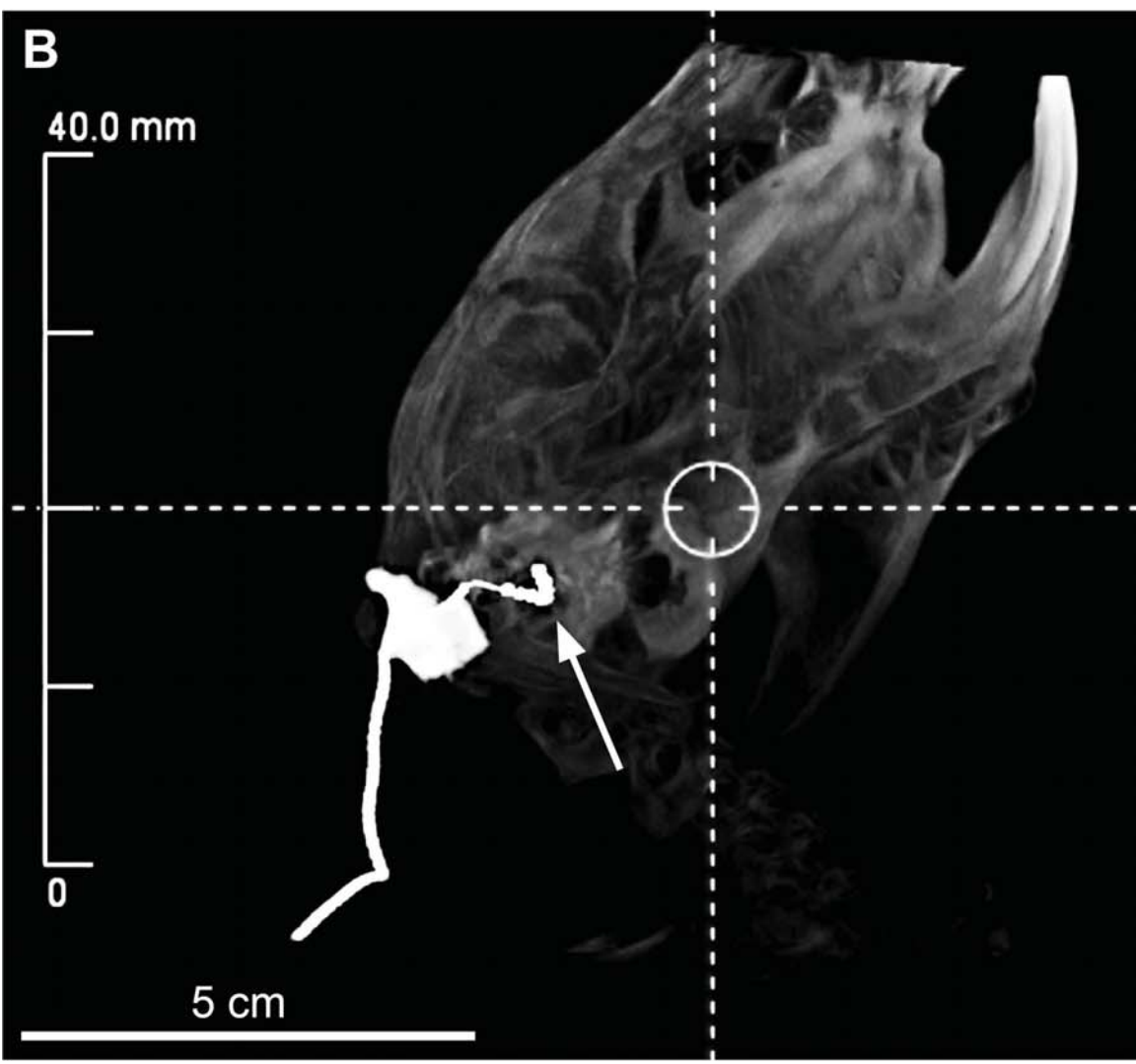
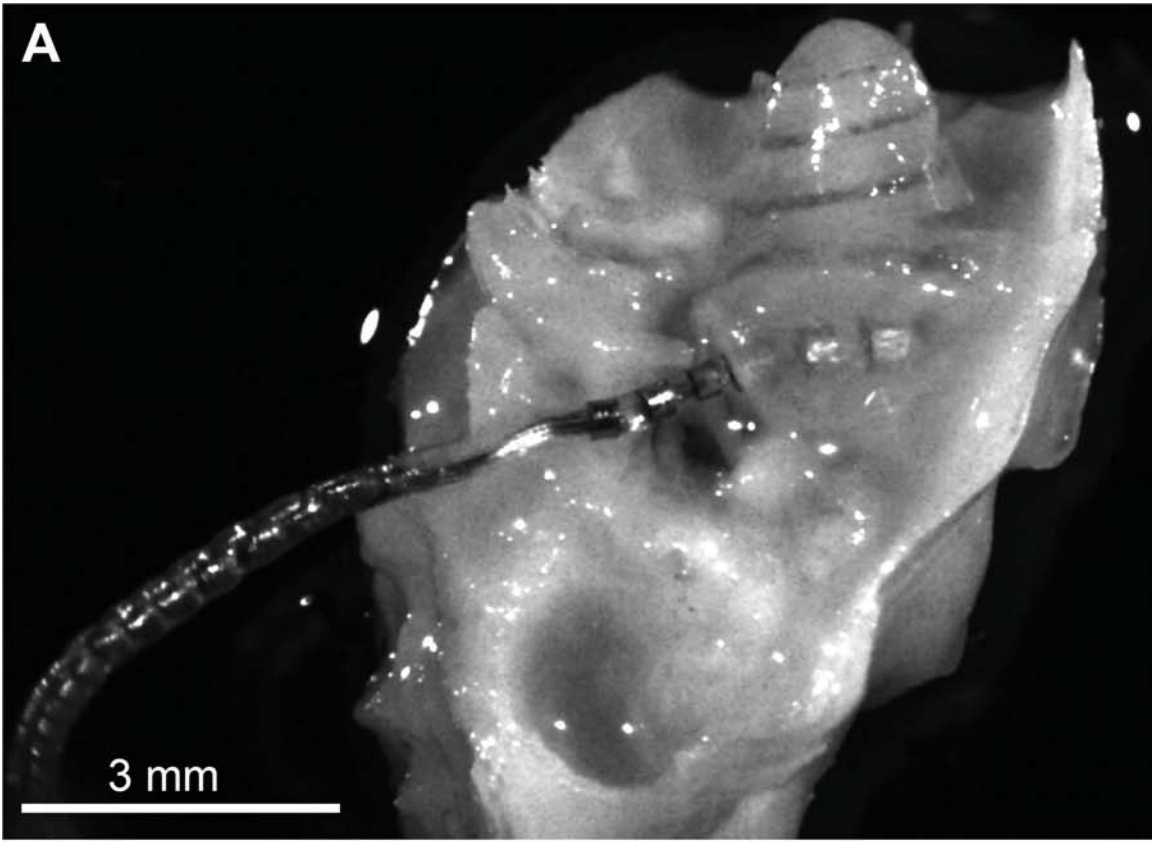
1476
1477
1478 interface beyond the previously reported two week time point ((Pinyon et al., 2014) Unpubl.
1479 data). n = 5 for control, n = 3 for BDNF gene augmentation. Box plot boundaries show 25%
1480 and 75% ranges for the control plasmid and upper and lower range for the neurotrophin group,
1481 solid line is median, dashed line = mean. Thresholds determined visually as shown in the
1482 previous figure. (100 μ s pulse width). BDNF data plasmid: pShuttle-CMVp-BDNFflag-IRES-
1483 GFPnls; GFP data plasmid: pShuttle-CMVp-IRES-GFPnls.
1484
1485
1486
1487
1488

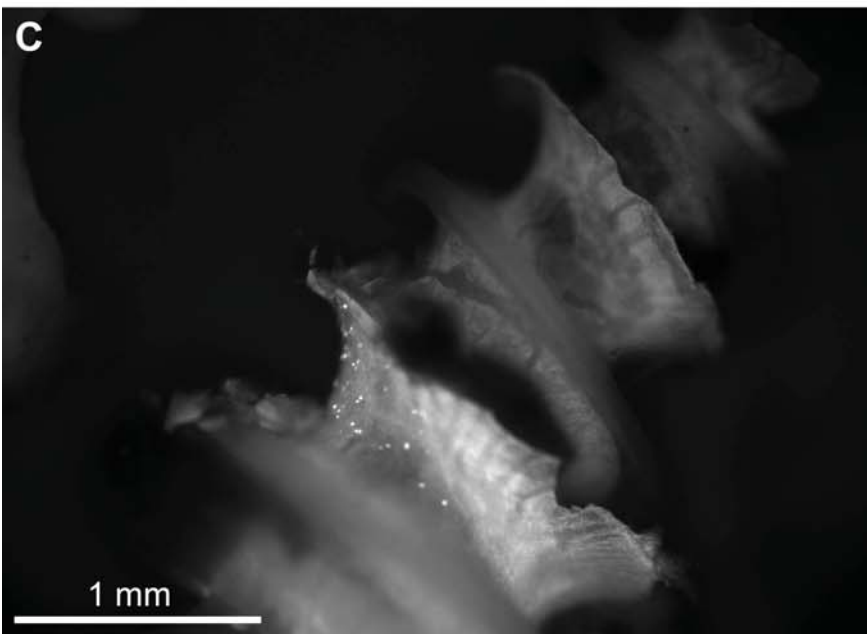
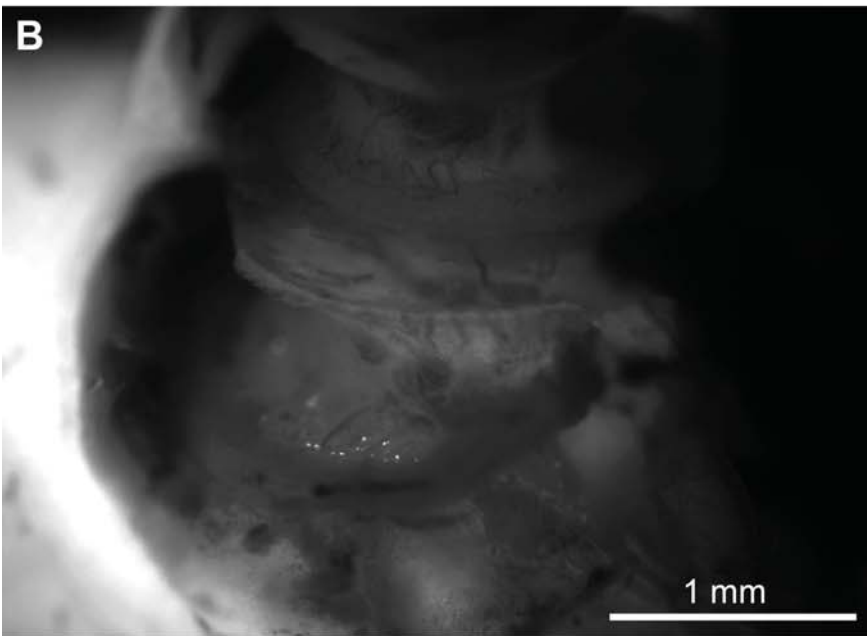
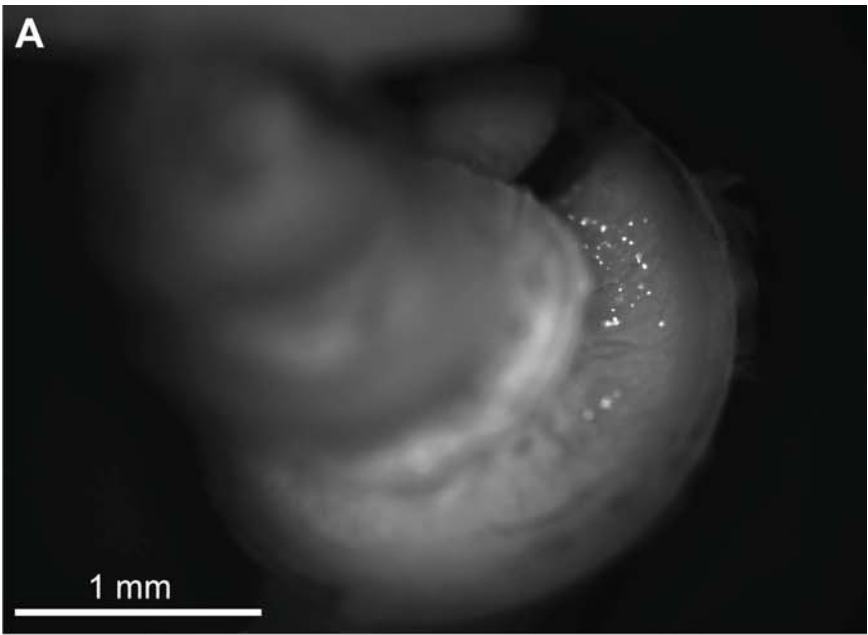
Fig. 9: Electric field modelling in silico of bionic array directed gene electrotransfer electric field maps based on an eight node cochlear implant electrode array. Modelling was undertaken based on a 50 μ l volume of saline (conductivity 1.5 S/m) stimulated with 4 V pulses using (A) ganged (four anodes (red), + four cathodes (blue) - ‘tandem’) electrode configuration and (B) ‘alternating’ polarity. Platinum-iridium electrode diameters 350 μ m, length 300 μ m, inter-electrode spacing 300 μ m). Top panels illustrate model geometry and stimulation configuration; In this model +4 V and -4 V were applied at the anodes and cathodes respectively. Centre panels show the field voltages arising from the two electrode array configurations, where the null point (0 voltage) extends orthogonally from the region between the + and - electrodes, or gangs of electrodes. Bottom panels display contour maps of the calculated electric fields. This highlights the point that it is not the absolute voltage that drives DNA electrotransfer, but the change in voltage over distance (electric field) which is greatest closest to the null points. We propose that cells experiencing electric fields in the 8-80 V/cm range will be transfected with DNA. Grey regions indicate the electric field is too weak to achieve electrotransfer.

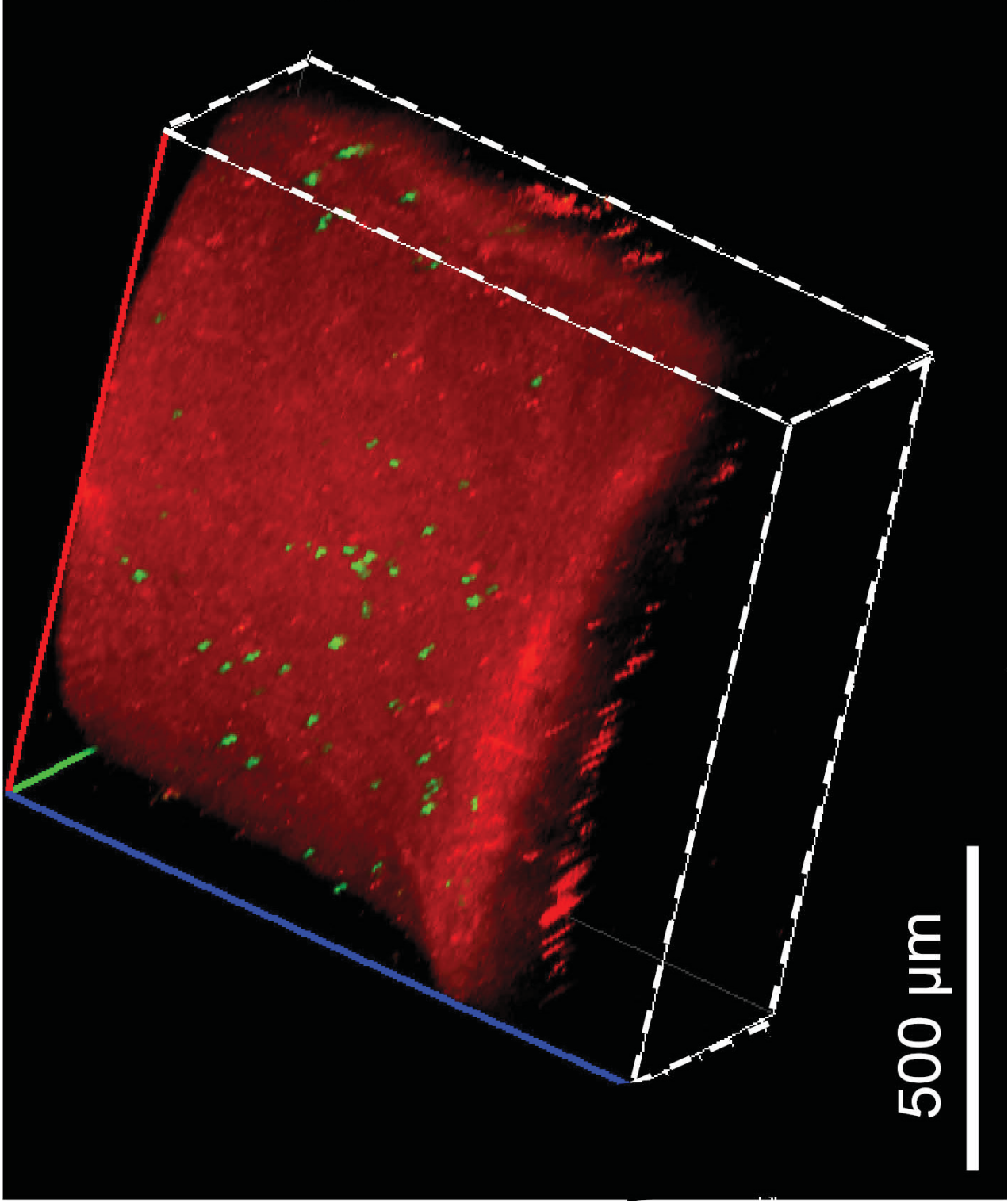
1513
1514
1515 **Fig. 10: Directed gene electrotransfer using HEK293 cell monolayers as a model for cochlear implant array-based electric field focusing.** Bionic array directed gene electrotransfer was performed in the HEK393 cell model using the cochlear implant eight-electrode array (shown as an overlay; anodes indicated as red + symbols and cathodes as black - symbols). The cells were grown on a round coverslip. Green spots indicate transfected cells expressing a GFP reporter gene detected using epifluorescence microscopy. Note that the cells are clustered in a circle around the mid-point of the array. This is centred on the null-point of the electric potential, but the highest electric field (greatest differential in field voltage with distance; see Fig. 9). In this example, +40V was applied to the anodes relative to the cathodes (5 x 50 ms pulses; Plasmid: pShuttle-CMVp-BDNFflag-IRES-GFPnls, 2 μ g/ μ l; four day cell culture post - DNA delivery).
1526
1527
1528
1529
1530
1531
1532
1533
1534

1535
1536
1537
1538
1539
1540
1541 **Fig. 11: GFP reporter expression confined to the basal turn region of the guinea pig**
1542 **cochlea after four days expression of the regulatory compliant pFAR4-CMVp-GFP**
1543 **miniplasmid in vivo.** The entire perilyphatic space was perfused with the naked DNA solution
1544 ((2µg / µl plasmid DNA, dissolved in Tris-buffered saline). The cochlear implant electrode
1545 array, modified as an acute gene delivery array where the four most internal electrodes acted
1546 as ganged anodes and the four basal electrodes as ganged cathodes ('tandem' configuration),
1547 was then inserted into scala tympani through the round window membrane (penetrating just
1548 the basal turn). A CUY21 electroporator (NepaGene, Japan) delivered 3 x 100 ms pulses of 30
1549 V to achieve the gene electrotransfer. The cochlear implant electrode array was removed
1550 immediately after the delivery of the pulse train. The image is a hemi-section view following
1551 decalcification of the treated cochlea. Note the green fluorescence signal is confined to the
1552 basal turn region where the gene delivery array was positioned. SV – scala vestibuli, ST – scala
1553 tympani, RM – Reissner's membrane.
1554
1555
1556
1557
1558
1559
1560
1561
1562
1563
1564
1565
1566
1567
1568
1569
1570
1571
1572
1573
1574
1575
1576
1577
1578
1579
1580
1581
1582
1583
1584
1585
1586
1587
1588
1589
1590
1591
1592
1593

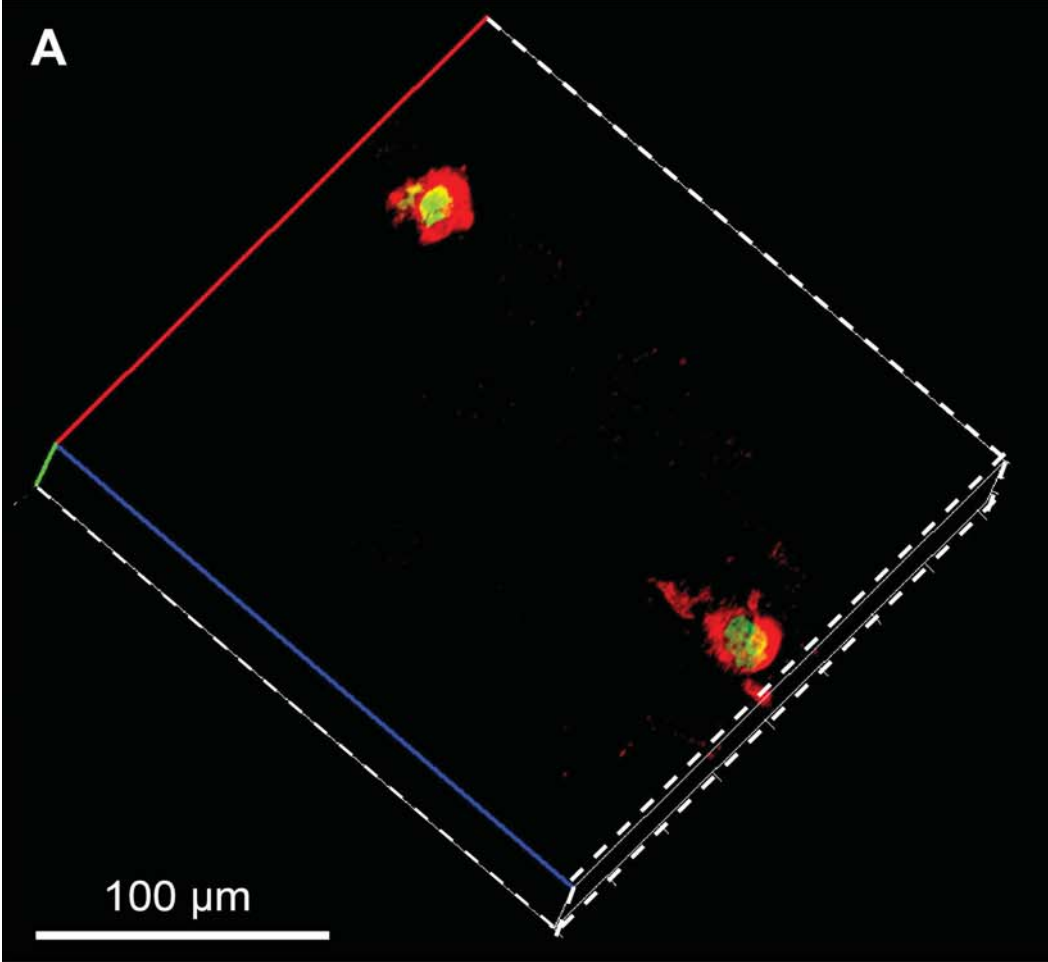




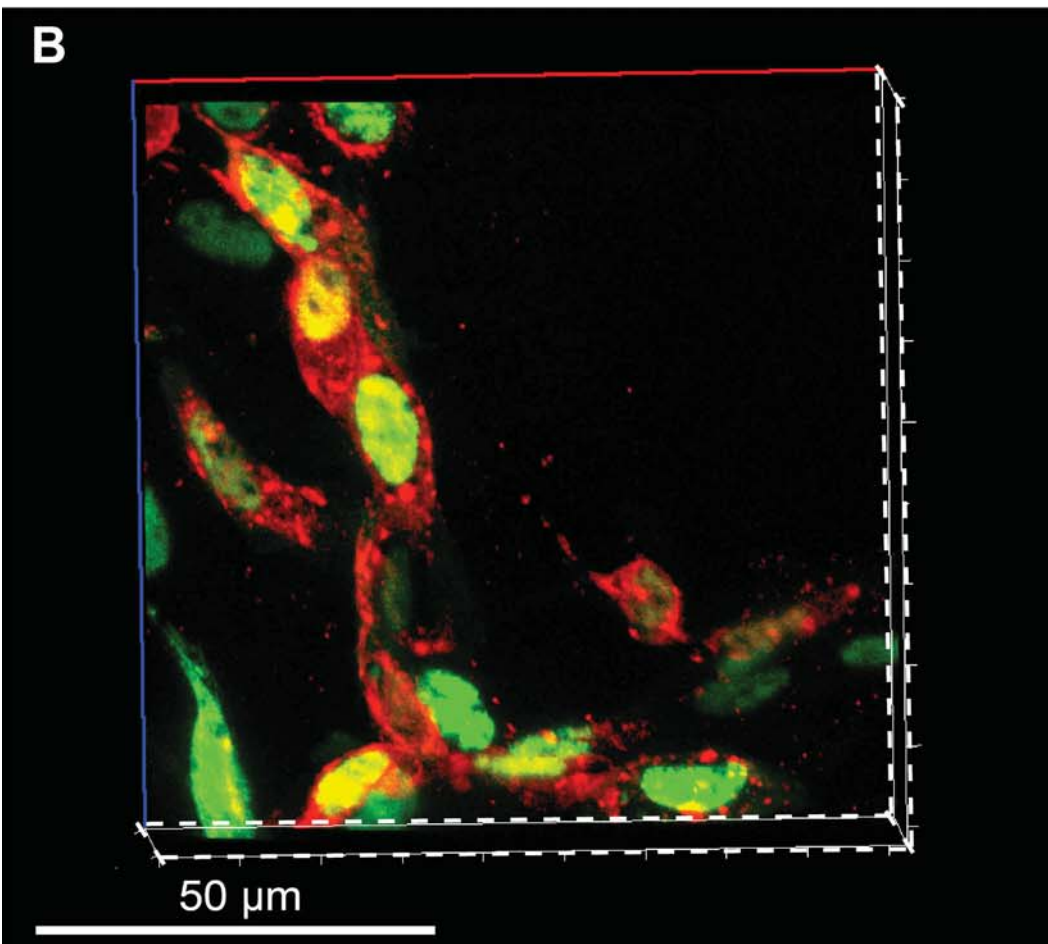


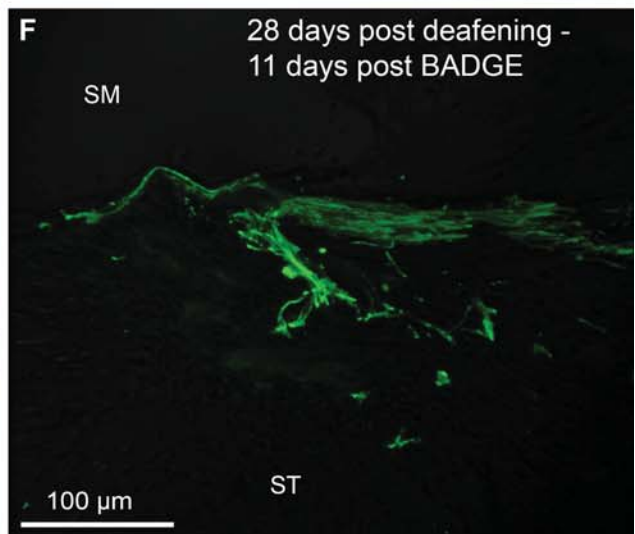
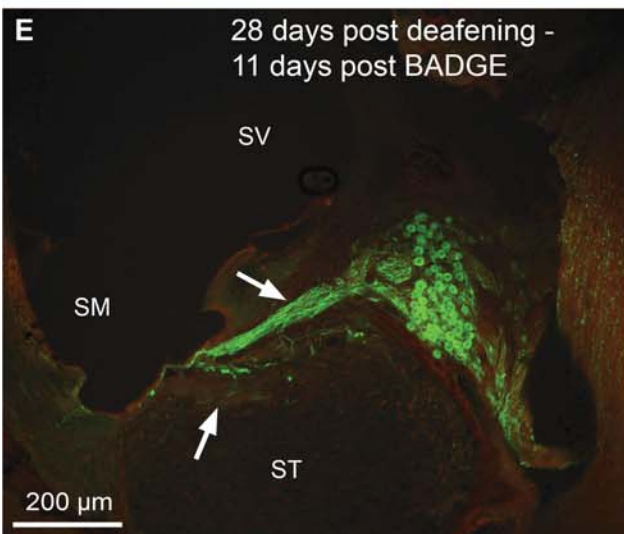
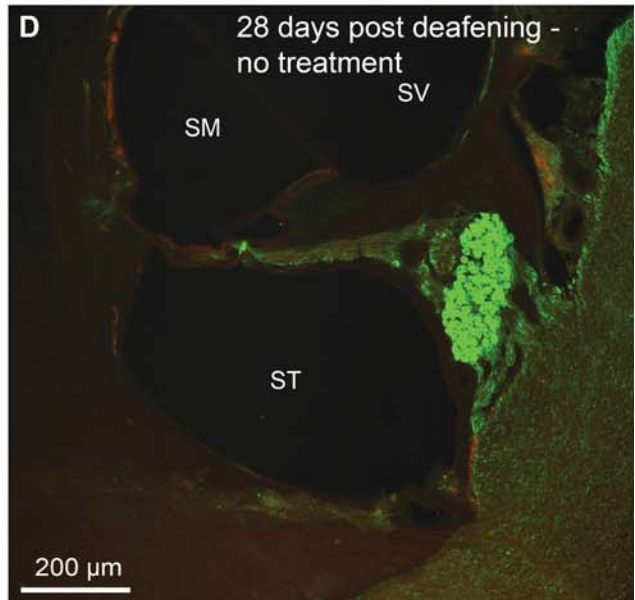
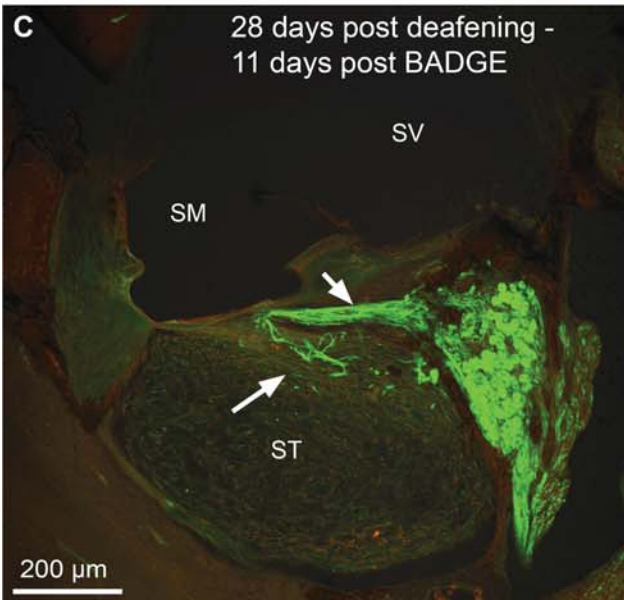
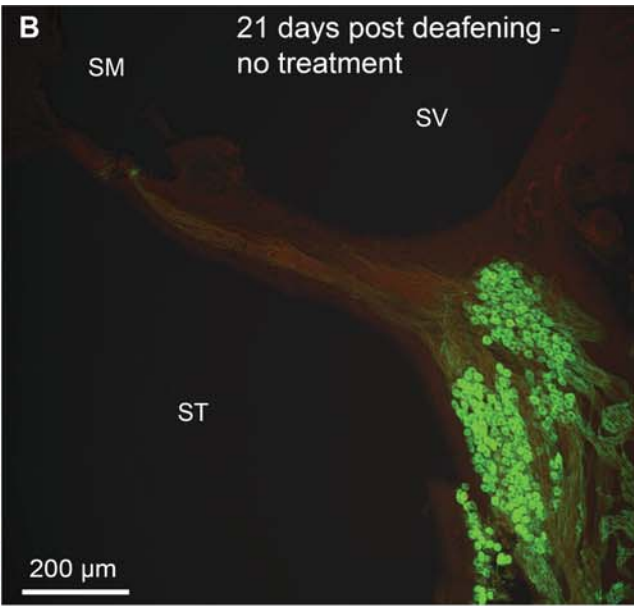
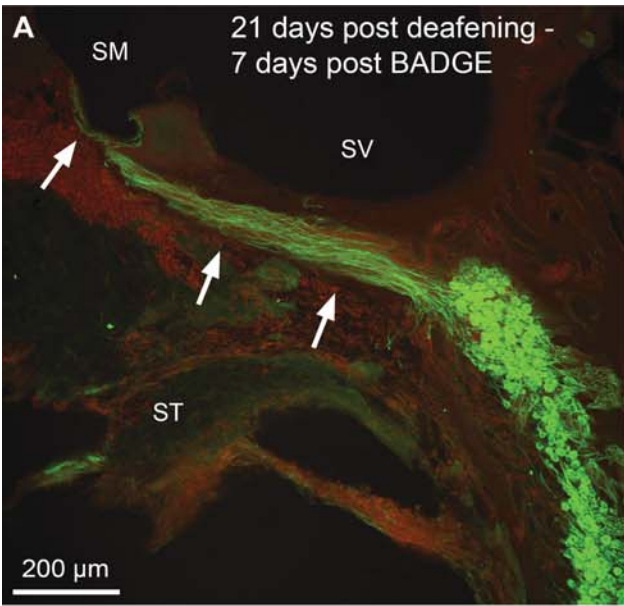


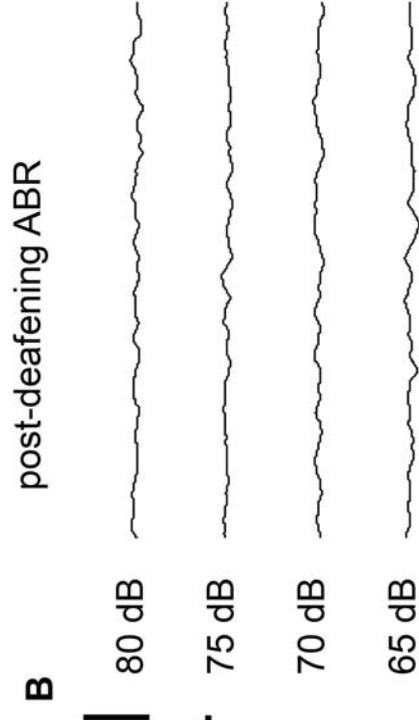
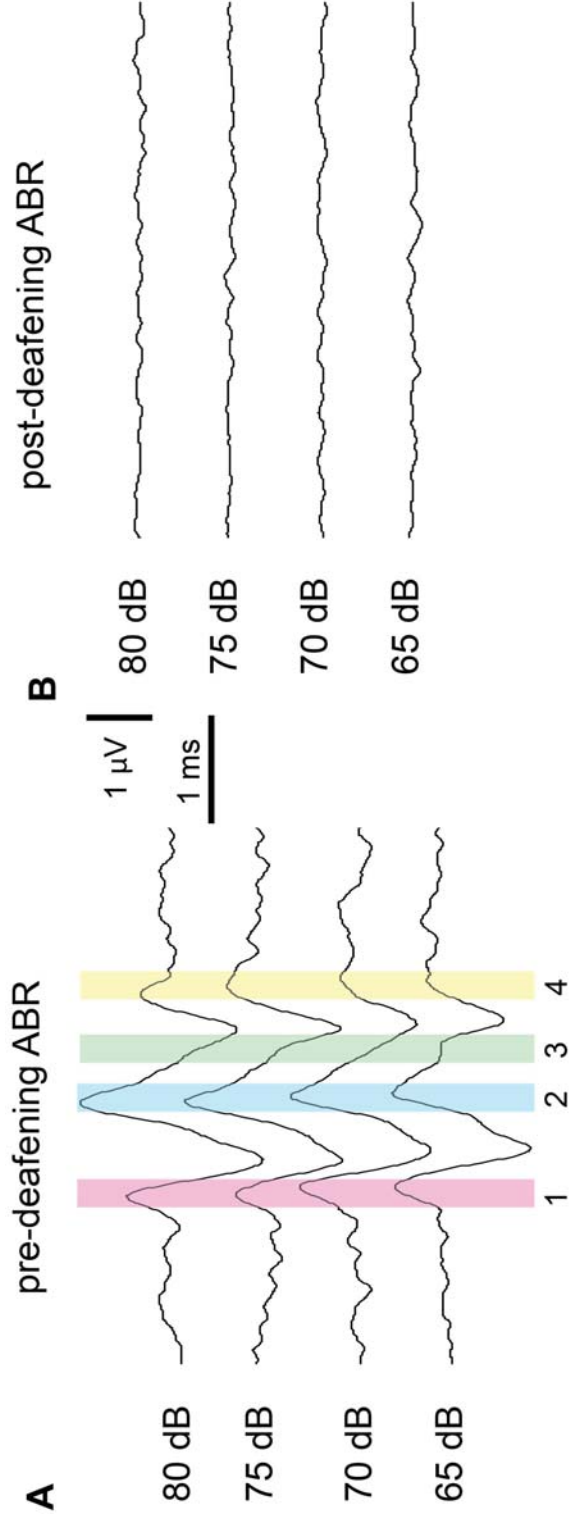
A



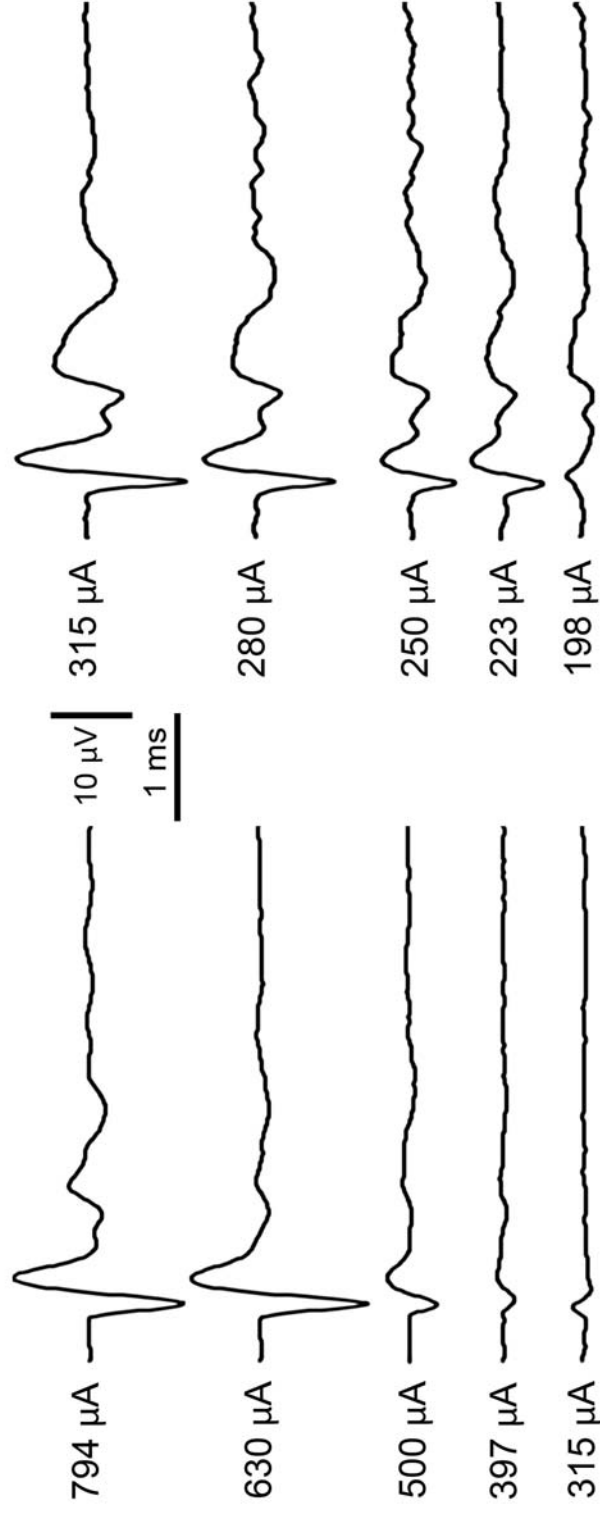
B



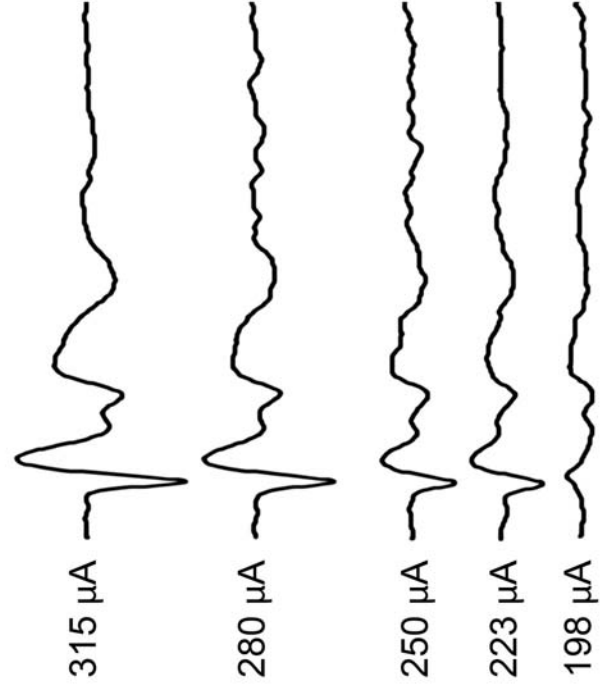


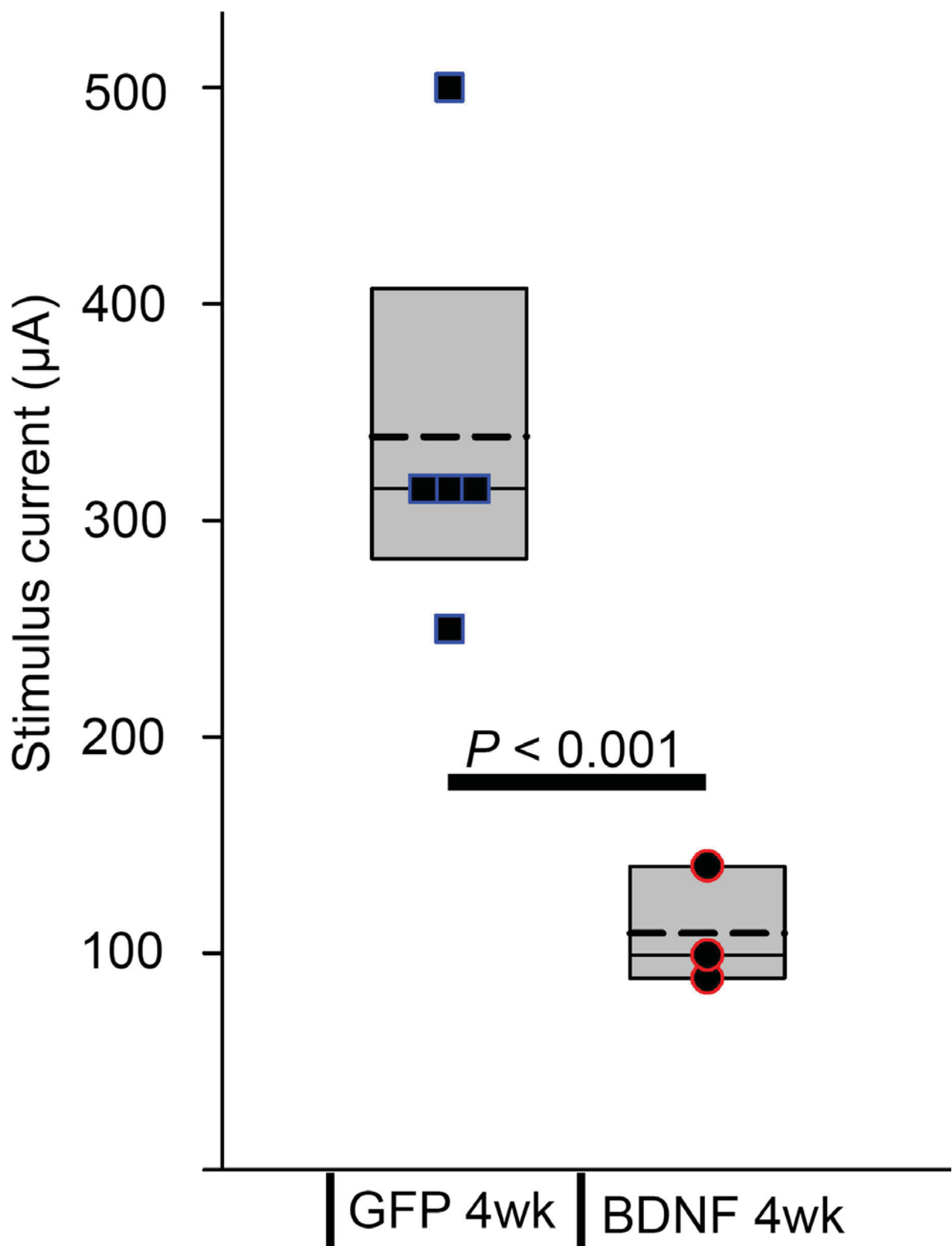


C post-deafening eABR without gene therapy

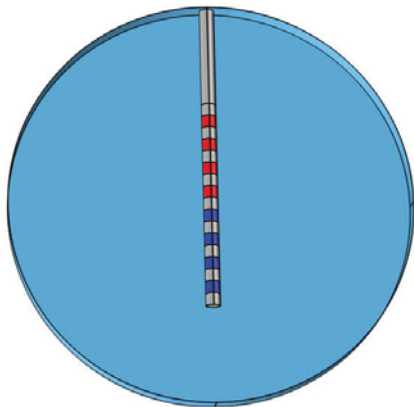


D post-deafening eABR with gene therapy

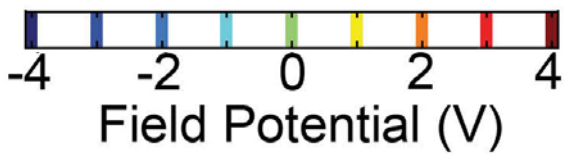
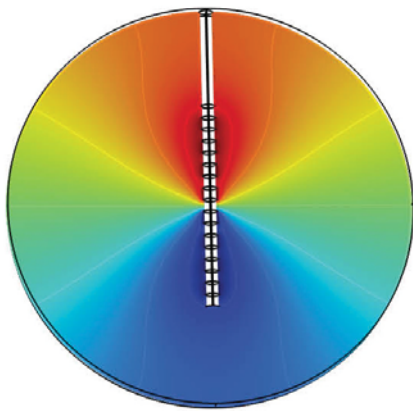




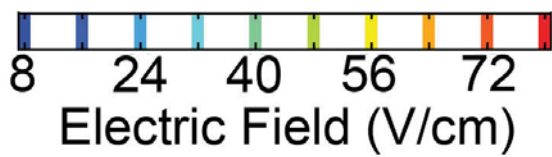
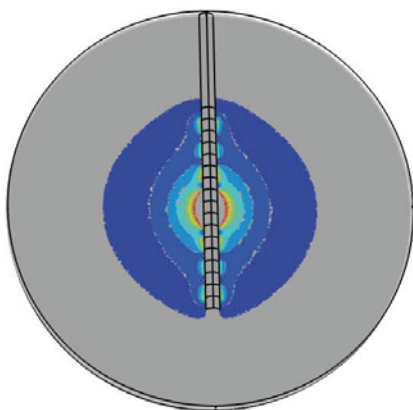
A Tandem



Electrode Configuration

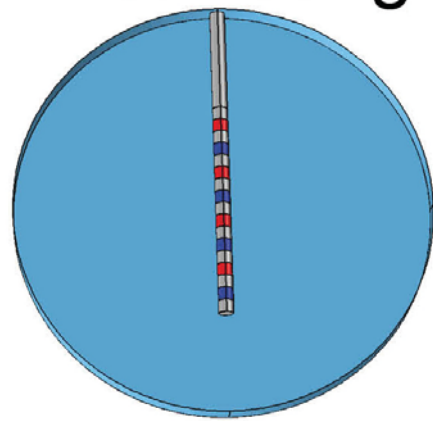


Field Potential (V)

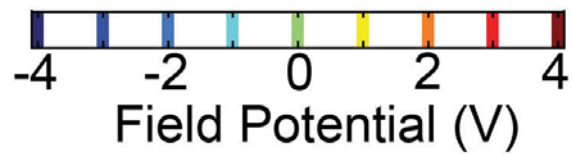
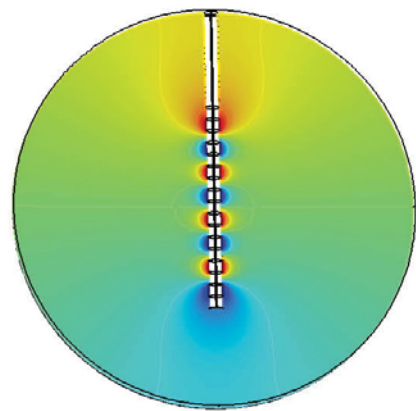


Electric Field (V/cm)

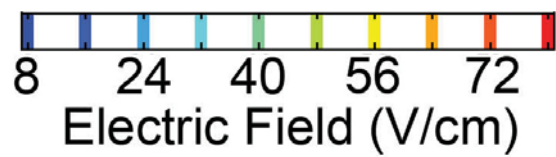
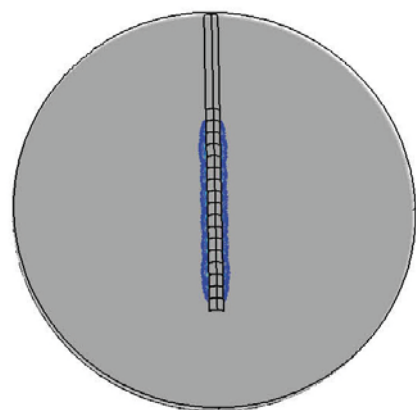
B Alternating



Electrode Configuration



Field Potential (V)



Electric Field (V/cm)

HEK293 cell
monolayer
40 V 5 x 50 ms
pulse

2 mm

